Palaeoenvironments and chronology of the Damvlei Later Stone Age site, Free State, South Africa

Michael Toffolo, Chantal Tribolo, Liora Kolska Horwitz, Lloyd Rossouw, Britt Bousman, Maïlys Richard, Elisabetta Boaretto, Christopher Evan Miller

Research Article

PALAEOENVIRONMENTS AND CHRONOLOGY OF THE DAMVLEI LATER STONE AGE SITE, FREE STATE, SOUTH AFRICA

MICHAEL B. TOFFOLO[1,2*], CHANTAL TRIBOLO[2], LIORA KOLSKA HORWITZ[3], LLOYD ROSSOUW[4,5], C. BRITT BOUSMAN[6], MAÏLYS RICHARD[2], ELISABETTA BOARETTO[7] & CHRISTOPHER E. MILLER[8,9]

[1]*Geochronology and Geology Program, Centro Nacional de Investigación sobre la Evolución Humana (CENIEH), Burgos, Spain*
[2]*Archéosciences Bordeaux, UMR 6034 CNRS, Université Bordeaux Montaigne, Pessac, France*
*(*Corresponding author. Email: michael.toffolo@cenieh.es)*
[3]*National Natural History Collections, Hebrew University of Jerusalem, Jerusalem, Israel*
[4]*Florisbad Quaternary Research Department, National Museum Bloemfontein, Bloemfontein, South Africa*
[5]*Department of Plant Sciences, University of the Free State, Bloemfontein, South Africa*
[6]*Department of Anthropology, Texas State University, San Marcos, USA*
[7]*D-REAMS Radiocarbon Dating Laboratory, Weizmann Institute of Science, Rehovot, Israel*
[8]*Institute for Archaeological Sciences and Senckenberg Centre for Human Evolution and Paleoenvironment (HEP), Eberhard-Karls-Universität Tübingen, Tübingen, Germany*
[9]*SFF Centre for Early Sapiens Behaviour (SapienCE), Department of Archaeology, History, Cultural Studies and Religion, University of Bergen, Bergen, Norway*

(Received May 2023. Revised September 2023)

ABSTRACT

The Modder River basin has been the focus of extensive surveys followed by targeted excavations of specific erosional gullies (known locally as dongas), where Middle and Later Stone Age artefacts and fossils are abundant. At Damvlei, a donga located on the left bank of the Modder, lithic artefacts and fossils were observed in the 1990s. Here, we present the results of two seasons of fieldwork (2019/21) at this locality, as well as unpublished surface faunal remains collected in 1995/96. Damvlei formed as a result of overbank deposition of the Modder River, as indicated by micromorphological analysis. The accumulation of the sedimentary sequence beneath the artefact-bearing levels started at 27 ± 3 ka at the earliest, based on optically stimulated luminescence dating. Artefacts, faunal remains, and phytoliths show that the site is characterised by Holocene Later Stone Age technology in an open-grassland environment typical of the terminal Florisian Land Mammal Age. Damvlei expands our knowledge of the Later Stone Age in the western Free State, and highlights the need for more extensive dating programmes aimed at framing human occupation in the central interior of South Africa.

Keywords: Later Stone Age, palaeoenvironment, alluvial, Free State, Modder River, Florisian.

INTRODUCTION

The occurrence of Pleistocene archaeological and palaeontological localities within exposed alluvial terraces in the Free State river drainages has been known for over 150 years (Cooke 1955). In some instances, the archaeological finds and fauna are clearly visible in exposed sections in the overbank sediments of the alluvial terraces, or else the material is found dispersed in erosional gullies ('dongas'). Published examples of such find locations include spots on the Schoonspruit in the north (Clark 1974; Brink & Rossouw 2000; Brink 2004; Brink *et al*. 2012; Toffolo *et al*. 2019; Bousman, Codron, *et al*. 2023), on the Riet River in the south (Berger & Brink 1996), and in the centre of the province on the Doring River (Brink *et al*. 1999), and Sand and Vet Rivers (De Ruiter *et al*. 2011). The most researched catchment is that of the Modder River, which features alluvial sites at Kranskraal (Van Hoepen 1932), Erfkroon (Churchill *et al*. 2000; Brink *et al*. 2016; Bousman, Brink, *et al*. 2023), Mitasrust (Rossouw 2006), Waterval (Trower 2010), and Lovedale (Richard *et al*. 2022; Wroth *et al*. 2022) (Fig. 1).

A major advantage of dongas over surface sites is that archaeological and palaeontological localities are embedded within stratified alluvial sequences, and so can be dated. This has been undertaken by using absolute dating methods such as optically stimulated luminescence (OSL) of quartz grains (Churchill *et al*. 2000; Tooth *et al*. 2013; Lyons *et al*. 2014; Wroth *et al*. 2022; Bousman, Brink, *et al*. 2023), while the presence of fauna has facilitated dating using electron spin resonance (ESR) of tooth enamel combined with uranium series dating (Brink *et al*. 2016; Richard *et al*. 2022). These methods have provided important chronological landmarks for Middle Stone Age (MSA) and Later Stone Age (LSA) human occupations in the open landscape of the Free State grasslands during the Late Pleistocene and early Holocene. In addition, some of the *donga* localities have produced palaeoenvironmental proxies such as phytoliths, which have facilitated the reconstruction of past vegetation. For instance, phytoliths indicated that a poorly known, pre-Howiesons Poort MSA industry recently dated to the late Marine Isotope Stage (MIS) 5 and early MIS 4 at Lovedale appeared during a dry period, thus raising the question of its relation to the coeval Still Bay technocomplex found at coastal sites (Lombard *et al*. 2022; Wroth *et al*. 2022). At Erfkroon, the early LSA contexts are among the latest in South Africa (Bousman & Brink 2018), and the site has yielded the only known Robberg lithic assemblage in the central interior (Palmison 2014). This is particularly important with regard to the human occupation of the Highveld grasslands during the Last Glacial Maximum (LGM), which has long been considered too dry to sustain permanent occupation due to insufficient plant diversity for human subsistence (Mitchell 1990, 2017).

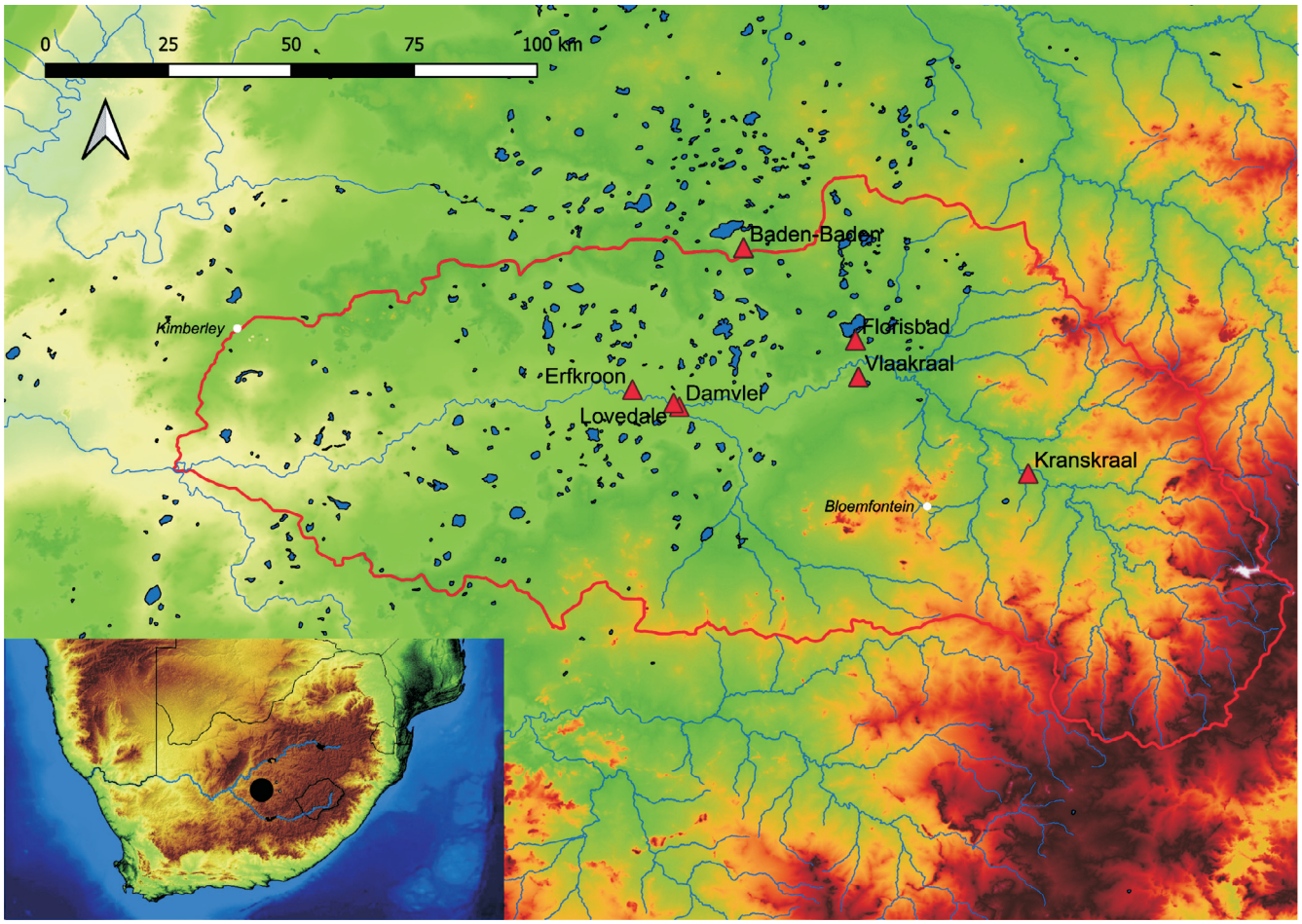

FIG. 1. *Location of Damvlei and other Middle and Late Pleistocene sites within the Modder River catchment (red outline), Free State. Blue patches represent salt pans. The inset shows the location of Damvlei in South Africa (black dot).*

Despite the clear archaeological and palaeontological potential of alluvial terraces, little research has been undertaken to date in terms of open-air LSA occupations in the interior of South Africa (Hallinan 2022). Besides Erfkroon, notable exceptions include small portions of the Doring River (Shaw *et al*. 2019), Tankwa Karoo (Hallinan 2021), Namaqualand (Dewar & Stewart 2017), Zeekoe Valley (Sampson 1985; Sampson *et al*. 2015), Orange River (Sampson 1970), Caledon River (Mitchell 2000), Wolwespruit (De la Peña & Witelson 2020), and Limpopo River (Le Baron *et al*. 2010). In order to better understand human occupation in the grasslands of the western Free State during the LSA, and possibly obtain a clearer picture of hunter-gatherer lifestyle and foraging strategies (e.g. specialised hunting) in an open-landscape where shelters and caves are not available, we excavated the find locality of Damvlei on the Modder River, located 11 km upstream of Erfkroon (Fig. 1). Damvlei was discovered in 1995 by L. Rossouw and J.S. Brink, who collected surface fossils and observed the presence of stone artefacts. This work was briefly mentioned in Brink and Henderson (2001). In 2018, M.B. Toffolo resurveyed the find locality, and conducted limited archaeological excavations in 2019 and 2021 together with L. Rossouw. In this paper we describe the formation processes of the Damvlei site in relation to the lithic artefacts, and propose a palaeoenvironmental reconstruction based on faunal remains and phytoliths. In particular, we used a micro-geoarchaeological approach to the study of sediments and fossils including infrared spectroscopy and micromorphology of sediments, which helped extract additional embedded information (e.g. Toffolo *et al*. 2017).

SITE DESCRIPTION AND EXCAVATION STRATEGY

The Modder is a meandering river flowing westwards through the Free State panfield, a region punctuated by seasonally dry lakes (salt pans) (Marshall & Harmse 1992; Barker 2011). The alluvial terraces of the Modder, formed at different stages during the Pleistocene, often include palaeontological and archaeological sites (Van Hoepen 1932; Churchill *et al*. 2000; Rossouw 2006; Wroth *et al*. 2022; Bousman, Brink, *et al*. 2023). Drops in the base level of the river, together with surface erosion of sandy sediments during thunderstorms, have favoured the incision of alluvial terraces and the formation of *dongas*, which exposed the sites (Tooth *et al*. 2013). For a detailed overview of the sedimentary context and geology of the area, see the description of the Lovedale donga, located 1.5 km downstream (Wroth *et al*. 2022).

Damvlei lies in a shallow donga located on the alluvial terrace on the left bank of the Modder River (28° 54′29.90″S, 25°41′51.94″E; 1215 masl), between the riverbed and a low-lying marshy ground (‘vlei’) created by the Kaalspruit, a seasonal tributary of the Modder (Fig. 2). Surface waters flow into the river through the vlei. At most locales the bluff separating the topsoil from the donga floor is between 1 and 2 m in height, although a few pinnacles exceed 2 m. Artefacts and fossils are scattered in great numbers on the surface of the donga bottom, but they could also be identified *in situ* within bluffs (Fig. 3). Considering that bones and artefacts were found eroding from the bluff within one metre from the topsoil, excavation trenches (1 × 1 m) were laid out at the top of the sequence, based on a surveyed grid system established for the excavation and anchored to a local beacon. All finds

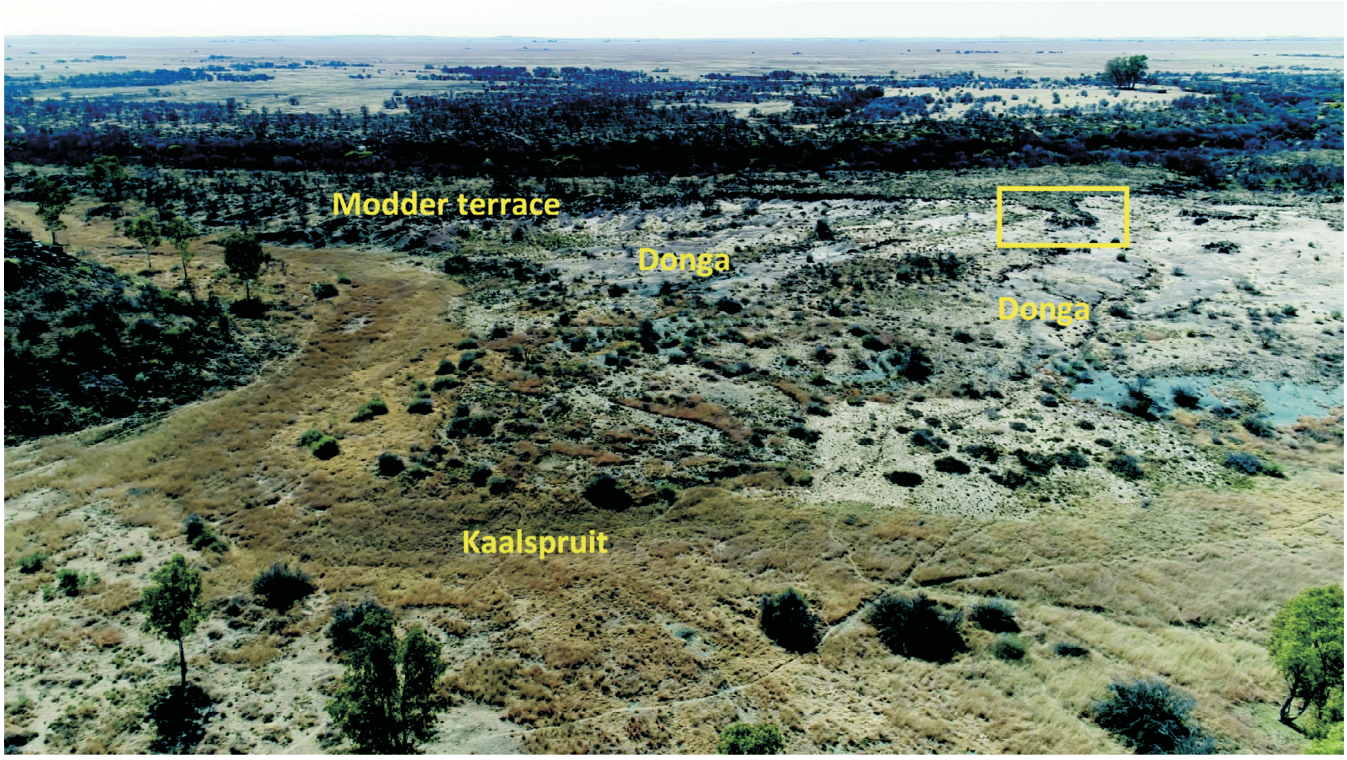

FIG. 2. *Aerial view of the Damvlei donga, showing the location of the Modder River (tree line in the background) and its alluvial terrace, the Kaalspruit vlei, and the excavation area (yellow box).*

were piece-plotted using a total station, including the eroded material collected from the surface. Units 1–4 are located at the tip of a preserved portion of alluvial terrace projecting within the donga, whereas Unit 5 was placed closer to the current riverbed (Fig. 4). Deposits were excavated in arbitrary 10 cm spits called Levels, down to a depth of 50 cm (70 cm in Unit 1), and all excavated sediment was dry-sieved through a 4 mm mesh. In addition, the bluff on the east side of Units 1–4 was cut

FIG. 3. *Eroded artefacts (foreground) lying on the donga floor at Damvlei.*

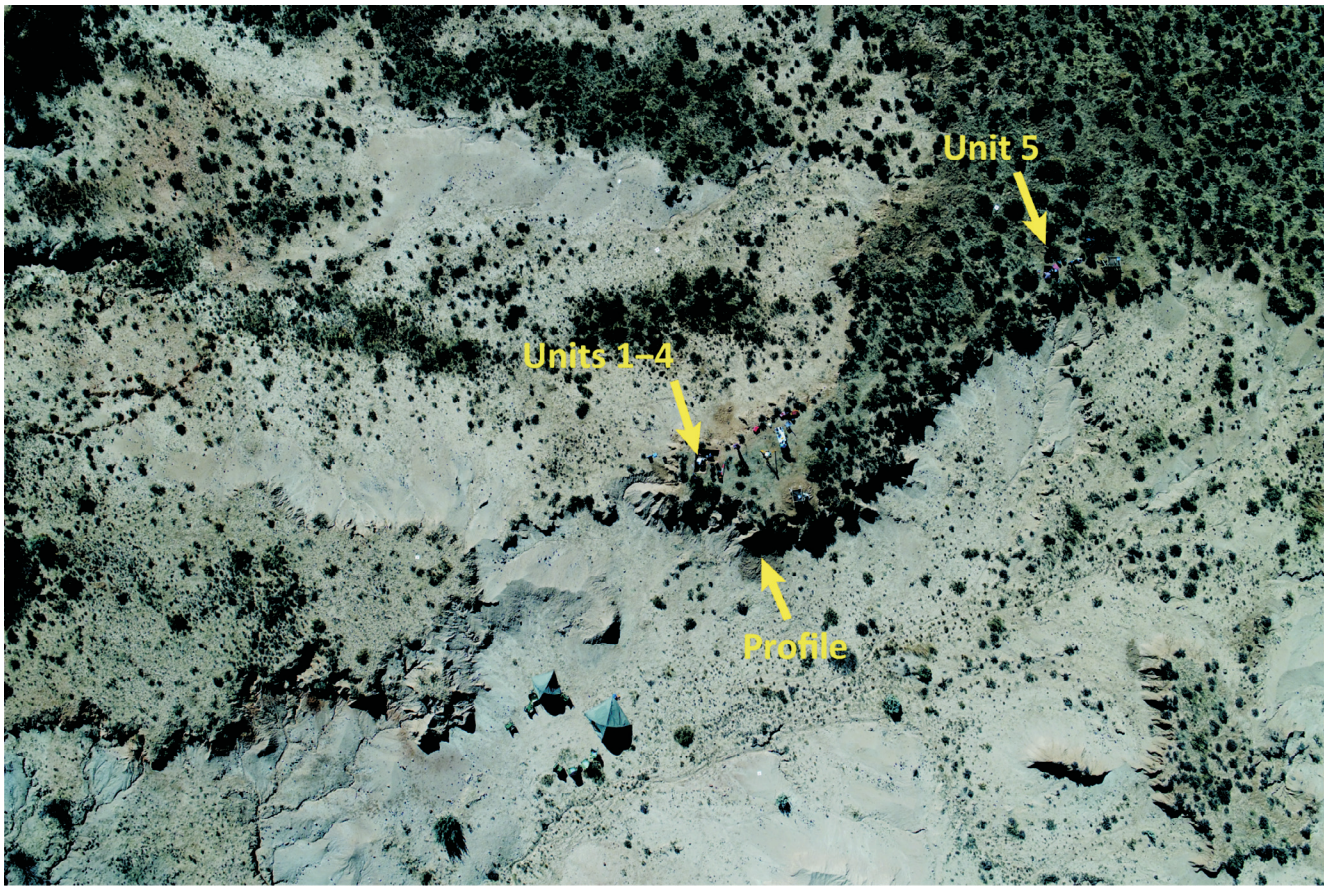

FIG. 4. *Aerial view of the Damvlei donga, showing the location of excavation areas and stratigraphic profile.*

back and straightened out to provide a profile showing the entire sequence down to the donga floor (Fig. 5). The stratigraphy includes two sedimentary units (SU). SU1 is a brown clayey sand about 2 m thick, with no visible sedimentary structures, which exhibits small (<1 cm across) pedogenic calcium carbonate nodules, concentrated in its lower portion. A red palaeosol about 30 cm thick, embedded within SU1, is visible at lower elevations in the bluff to the south of Units 1–4, and can be traced within the donga (Supplementary Fig. 1). The depth of the palaeosol was not reached in the stratigraphic profile. Above SU1, SU2 is a light-brown sandy sediment, about 20 cm thick, with cross-bedding visible in places. The boundary between the two units is sharp (Fig. 6).

MATERIAL AND METHODS

FOURIER TRANSFORM INFRARED SPECTROSCOPY (FTIR)

Sediments (n = 20) and bones (n = 8) were analysed with FTIR to determine their composition and state of preservation. Samples were powdered in an agate mortar and pestle and about 5 mg of each were mixed with 40 mg of KBr and pressed into 7-mm pellets using a hand press. Infrared spectra were collected in transmission mode after 32 scans within the 4000–400 cm^{-1} spectral range using a Thermo Scientific Nicolet iS5. Spectra were analysed using OMNIC 9.13 and Macros Basic 10, and phases were identified using the infrared spectra library of the Kimmel Center for Archaeological Science, Weizmann Institute of Science (https://centers.weizmann.ac.il/kimmel-arch/infrared-spectra-library), and standard literature (Farmer 1974; Van der Marel & Beutelspacher 1976). The degree of atomic order of carbonate hydroxyapatite in bones was determined following the method of Asscher *et al*. (2011). To identify heat-altered clay minerals in the archaeological sediments, we used as a reference a termite mound burned during a controlled veld fire at Florisbad (40 km NE of Damvlei), which reached temperatures exceeding 600°C (Gowlett *et al*. 2017). Sediment colours ranged from black to brown and bright red, depending on exposure to different temperatures (Supplementary Fig. 2). In addition, we prepared a reference database of heated sediments collected from the topsoil at Florisbad to monitor changes in the infrared spectrum of clay minerals at different temperatures (Berna *et al*. 2007). Sediments were heated to 300, 400, 500, 600, 700 and 800°C in an electric muffle oven in air atmosphere for 4 h, and analysed with FTIR following the procedure described above.

MICROMORPHOLOGY OF SEDIMENTS

One block of intact sediment was collected at the transition between SU1 and SU2 to determine the formation and post-depositional processes of the site. The block was carved out of standing sections and jacketed in plaster for transport to the Institute for Archaeological Sciences at the University of Tübingen, where it was dried at 40ºC in an oven for one week, embedded in a mixture of polyester resin and styrene (70:30) catalysed with MEKP, and left to solidify under a fume hood. The solid block was sliced into a 2–3 cm-thick slab with a large rock saw and then further cut down into ~6× 8 cm chips with a tile saw. The chips were processed at the thin section laboratory of the CENIEH, where they were mounted on glass slides and polished to a thickness of 30 μm. Thin sections (n = 2) were analysed using a petrographic microscope at different magnifications up to ×400. Descriptions and analyses are based on established literature (Macphail & Goldberg 2017; Stoops *et al*. 2018; Stoops 2021).

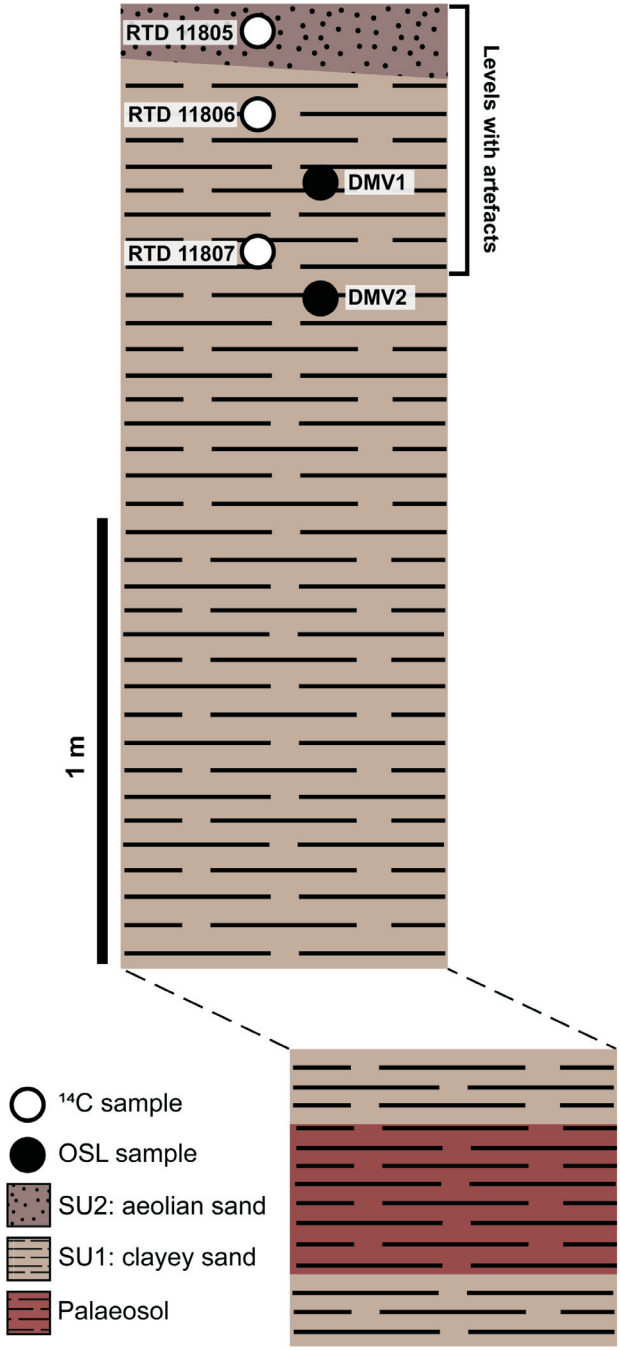

FIG. 5. *Damvlei stratigraphic sequence exposed in the* donga *profile, showing the location of radiocarbon (^{14}C) and OSL dating samples. All dating samples were collected in the excavation trench of Units 1–4 except for DMV1, which was collected from the stratigraphic profile. The red palaeosol, visible at other locales in the* donga, *was not reached in the stratigraphic profile.*

PHYTOLITH ANALYSIS

Phytoliths were extracted from bulk sediment samples collected from each level of Unit 1 (n = 6) and from the red palaeosol (n = 1), and counted following the method of Katz *et al*. (2010), to determine the proportions of C_3 and C_4 grass short-cells and thus shed light on local temperature and moisture availability. Morphotypes were identified at ×200 and ×400 magnifications using a petrographic microscope and described following the International Code for Phytolith Nomenclature 2.0 (Neumann *et al*. 2019) and standard literature (Mulholland & Rapp 1992).

FAUNAL ANALYSIS

All animal remains were encrusted with a hard calcium carbonate matrix resulting from leaching of water and were cleaned with a dilute acetic acid solution to facilitate identification. The underlying bone was not well preserved with both enamel and bone showing cracking and exfoliation (weathering stage D according to Behrensmeyer 1978). Identifications were undertaken using the comparative zoological collection of the Florisbad Quaternary Research Station. Measurements (in mm) follow Von den Driesch (1976). Bovid size classes are based on Brain (1974).

OSL DATING

Two bulk sediment samples were collected for OSL dating at 40 cm (stratigraphic profile, DMV1, same depth as Level 4) and 65 cm (Unit 1 Level 7, DMV2) beneath the surface. While bioturbation was visible in the field, collection was restricted to locations that appeared less affected by faunal activity. Samples

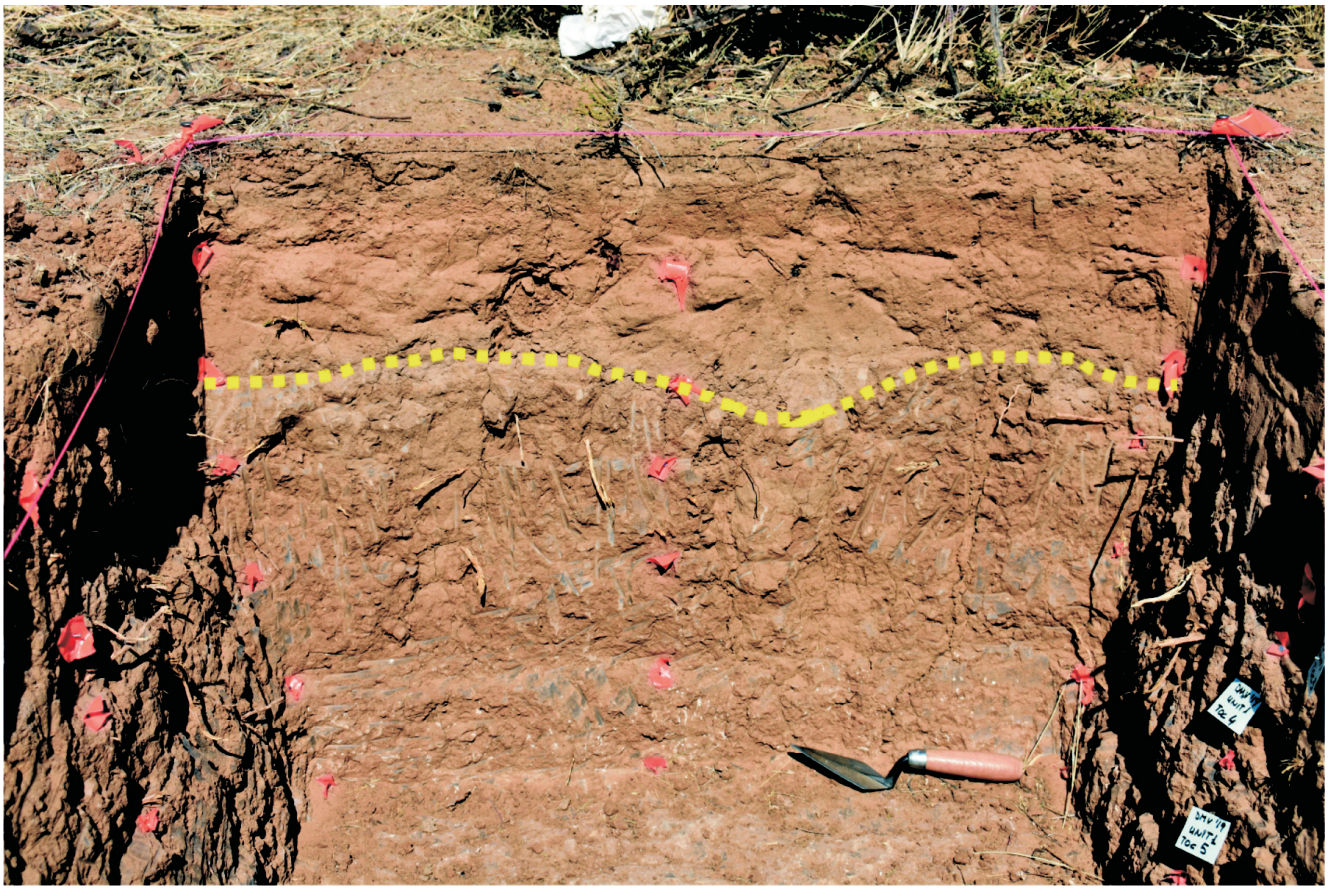

FIG. 6. *East section of Unit 1 at the end of the 2019 season. Orange flagging tape marks levels every 10 cm. Note the sharp boundary between SU1 and SU2 at 20 cm depth (dotted line), and the appearance of small calcium carbonate nodules at 50 cm depth (trowel = 20 cm).*

were collected at night under subdued orange light and placed in lightproof bags, after removing the surface previously exposed to sunlight. The gamma dose rate was measured with a field gamma-ray spectrometer multichannel analyser connected to a NaI(Tl) detector (Inspector 1000, Canberra). The gamma dose rate was obtained for each sample following the "threshold" technique (Mercier & Falguères 2007).

Samples were processed following the protocol used for similar samples from Lovedale, located 1.5 km to the NW of Damvlei (Wroth *et al*. 2022). Quartz grains in the 100–140 μm size fraction were extracted through wet sieving, chemical treatment with HCl (10%) and H_2O_2 (30%), and separation with LST (heteropolytungstate) at 2.72 and 2.62 g/cm^3. Finally, HF etching (40% for 60 min) was followed by HCl (10%) treatment. The grains were mounted on single grain discs displaying 100 holes, 150 μm large and 150 μm deep. An infrared stimulated luminescence (IRSL) test (Duller 2003) suggested the prepared samples were free of contaminating feldspar grains. Equivalent dose measurements were performed with a Risø TL DA 20 device (excitation: 532 nm, 10 mW, Nd:YVO4 diode-pumped laser; detection: 7.5 mm Hoya U340 filter in front of a PDM 9107Q-AP-TTL-02 photo-multiplier tube with 280–380 nm range; irradiation with a 90Sr-90Y beta source delivering *ca* 0.1 Gy/s) (Bøtter-Jensen *et al*. 2000). Analyses were run with Analyst v.4.57 (Duller 2015).

Linearly modulated OSL measurements were performed on DMV1. The signal was compared to the signal of the Risø calibration quartz (Hansen *et al*. 2015), and it was concluded that it was dominated by a fast component. Then, the Single Aliquot and Regenerative dose protocol (SAR; Murray & Wintle 2000) was applied (Supplementary Fig. 3). Growth curves were fitted with an exponential such as $Lx/Tx = a(1-\exp\left(\frac{D+c}{D_0}\right))$, where Lx/Tx is the normalised luminescence signal, a, c, and D_0 are the fitting parameters, and D is the dose. Grains were selected based on their sensitivity (natural test dose signal >3 sigma above background level; maximum relative natural test dose error <10%), their recuperation signal (Lx/Tx after a zero Gy dose <5% of the Lx/Tx signal for the highest regenerative dose), and their saturation value (D_0 threshold, Thomsen *et al*. 2016). A dose recovery test (Supplementary Fig. 4) allowed us to conclude that the protocol was efficient for recovering a laboratory given dose of 22–25 Gy (dose recovery ratio of 0.96 ± 0.02 ad 1.00 ± 0.02 for DMV1 and DMV2, respectively) (Supplementary Fig. 4 and Supplementary Table 1).

The dose rate is the sum of the contribution from the cosmic, gamma, and beta dose rate. The alpha dose rate was neglected because of the HF etching. The cosmic dose rate was calculated using the equation of Prescott and Hutton (1994), applying the current burial depth. The beta dose rate was calculated from the U, Th, and K contents of the samples. Those were determined with High Resolution Gamma Spectrometry. Conversion factors of Guérin *et al*. (2011) and attenuation factors of Guérin *et al*. (2012) were applied. Since the fluctuation in water content might have been important while the past mean water content is unknown, a mean water content of 50 ± 15% of the estimated saturation level (30%) was applied.

RADIOCARBON DATING

Sediment samples (n = 3) were collected from Unit 1 to extract total organic carbon (TOC) for radiocarbon dating. Sediments were treated with 1M HCl to eliminate carbonates. The weight of the sediment was recorded before and after the

acid treatment to calculate the percentage of carbonates. After this step about 0.5 g (samples were precisely weighed) were introduced in a quartz ampule with CuO, evacuated and heated to 900° C for 4 hours to oxidise organic matter to CO_2. The extracted CO_2 was graphitised using an EA-AGE3 system, composed of an elemental analyser (EA, 'vario ISOTOPE SELECT' by Elementar), coupled to a third generation of the Automated Graphitization Equipment (AGE3, Ionplus). Carbon stable isotopes ratios ($\delta^{13}C$) were measured for each sample. The ratio between ^{14}C and the stable isotopes ^{12}C and ^{13}C as graphite was measured using the accelerator mass spectrometer at the D-REAMS Radiocarbon Dating Laboratory, Weizmann Institute of Science (Regev *et al*. 2017). All radiocarbon ages were corrected for isotopic fractionation, calibrated using OxCal 4.4 and the SHCal20 atmospheric calibration curve for the southern hemisphere (Bronk Ramsey 2009; Hogg *et al*. 2020).

RESULTS

FIELDWORK

The 2019/21 seasons produced a total of 262 lithic artefacts and two bone fragments from Units 1–5 (Table 1), with additional 37 lithic artefacts and 78 faunal remains collected from the surface of the donga. Most of the tools from the excavation are made on hornfels characterised by a light grey patina, and show features and typologies consistent with LSA reduction strategies. Cryptocrystalline silicate (chalcedony, jasper) is the second most represented raw material for tools, followed by dolerite and petrified wood. Edge-modified flakes, core flakes/bladelets, and scrapers are the most represented tool categories (Table 2). Most artefacts were unearthed from Levels 3–5 (20 to 50 cm depth). Artefacts in Level 1 include microlithic flakes and tools that can be associated with the Wilton technocomplex, such as 'thumbnail' scrapers. Levels 2–6 include much larger flakes and tools such as scrapers of the Lockshoek industry, the regional variant of the Oakhurst technocomplex (Lombard *et al*. 2022).

Both Oakhurst and Wilton technocomplexes are represented in the surface collection. Most of the surface tools are made on hornfels characterised by a dark brown to silvery black patina, followed by cryptocrystalline silicates and quartz, with bladelet cores and scrapers the most represented tool categories (Table 3). It should be noted that unmodified dolerite cobbles, observed in large quantities on the surface but not collected, are ubiquitous and always associated with flakes and tools made of other rock types. A few surface microliths might belong to the earlier Robberg technocomplex, although no unequivocal evidence is currently available. Notable surface finds include points, fragments of ochre, and a few flakes and unworked slabs of banded ironstone (Fig. 7). None of the artefacts recovered at the site show signs of rolling or long-distance transportation by water. The detailed analysis of the full lithic assemblage will be made available at a later stage.

TABLE 1. *Number of lithic artefacts by Level in each Unit. Dash indicates unexcavated level.*

Level	Unit 1	Unit 2	Unit 3	Unit 4	Unit 5	Total
1	11	6	0	0	3	20
2	10	17	5	3	4	39
3	28	27	10	6	3	74
4	9	8	35	5	5	62
5	13	18	8	0	24	63
6	4	–	–	–	–	4
7	0	–	–	–	–	0
Total	75	76	58	14	39	262

FTIR

The alluvium of SU1 is composed of a mixture of clay minerals of the kaolinite and smectite groups (3696, 3620, 1036 cm^{-1}), quartz (1163, 1086, 797, 779, 695, 515, 462 cm^{-1}), and feldspars (646 cm^{-1}). This composition is common in the sediments and soils of the region, as was shown at Lovedale and Florisbad (Toffolo *et al*. 2017; Wroth *et al*. 2022). The proportions of these components change in SU2, where quartz sand becomes dominant and clay minerals nearly disappear.

Small aggregates of black and red clay recovered from SU1 (Unit 2, Level 5) exhibit signs of exposure to elevated temperatures, such as the disappearance of the Al–O-H absorption bands of clay minerals in the 4000–3500 cm^{-1} region, and the shift of the Si-O-Si band to higher wavenumbers (1043 cm^{-1} in the black clay, 1051 cm^{-1} in the red clay) (Berna *et al*. 2007). These results are supported by comparison with the burnt termite mound sampled at Florisbad, where the red colour corresponds to the largest shift of the Si-O-Si band (overlap with the quartz band at 1086 cm^{-1}) and thus to the highest temperature reached during burning (Fig. 8). In addition, based on the reference database of heated sediments from Florisbad, the band shift in the red clay can be associated with temperatures exceeding 600°C (Supplementary Fig. 5). This is further confirmed by the analysis of two fragments of bone found together with the heat-altered clay aggregates, which exhibit a high splitting factor of carbonate hydroxyapatite (6.1 and 6.5) and a small band at 630 cm^{-1}, typical of exposure to tempera-

TABLE 2. *List of raw materials divided by category of excavated tool (CCS: cryptocrystalline silicate).*

Excavated tool	CCS	Dolerite	Hornfels	Petrified wood	Total
Adze			2		2
Backed bladelet				1	1
Backed bladelet – medial discard			1		1
Bipolar piece			2		2
Core – bladelet	2		2	1	5
Core – flake	1		4		5
Core – fragment			1		1
Edge modified flake			11		11
Groundstone		1			1
Hammerstone		1			1
Scraper – end	2		3		5
Scraper – fragment			1		1
Scraper – side			1		1
Total	5	2	28	2	37

TABLE 3. *List of raw materials divided by category of surface tool (CCS: cryptocrystalline silicate).*

Excavated tool	CCS	Hornfels	Quartz	Total
Bipolar piece		1	1	2
Core bladelet	2	1	1	4
Groundstone		1		1
Point		1		1
Reamer		1		1
Scraper – circular		2		2
Scraper – end	1			1
Scraper – side		1		1
Total	3	7	2	13

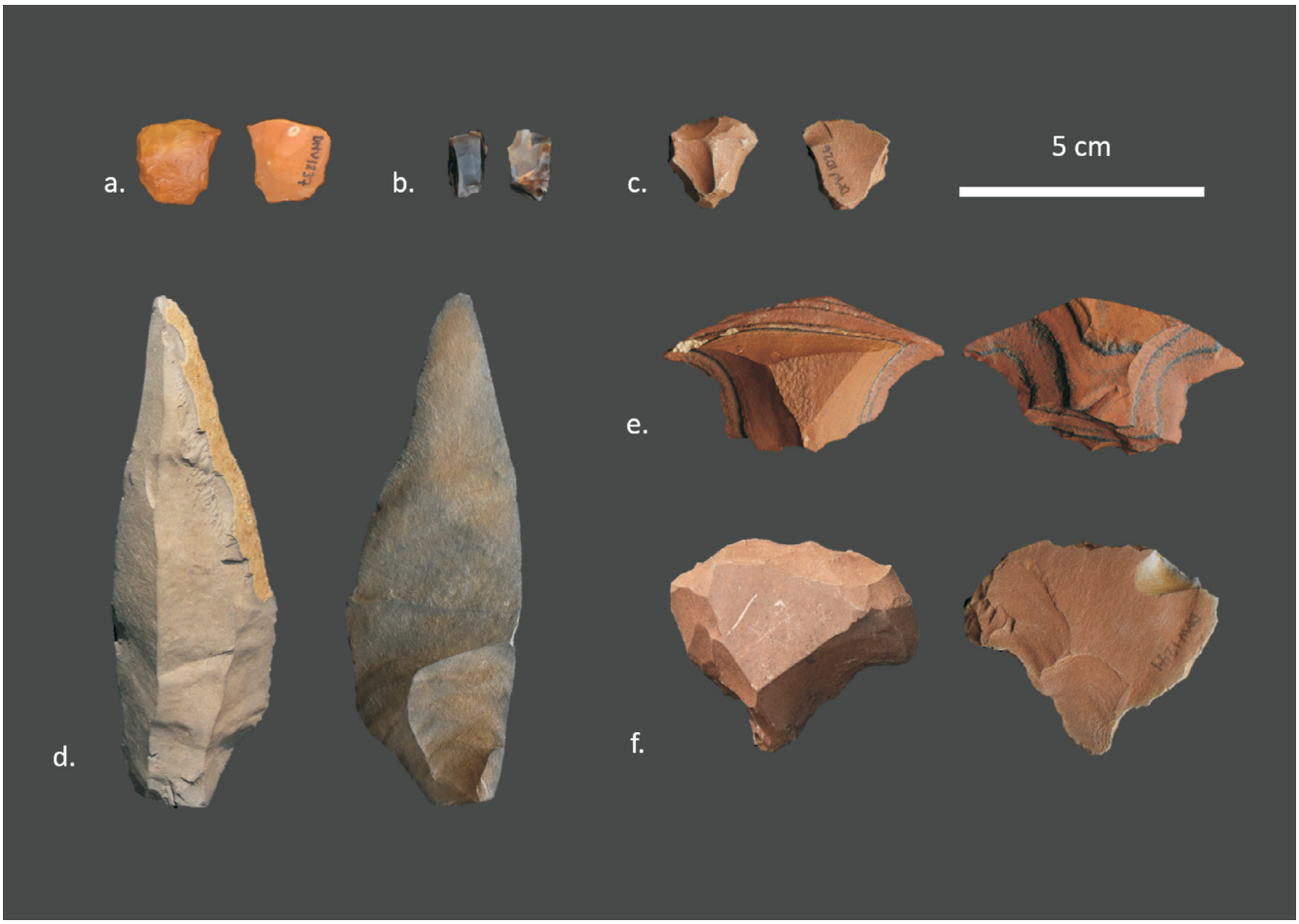

FIG. 7. *Representative lithic artefacts recovered at Damvlei:* (**a**) *end-scraper from surface, cryptocrystalline silicate;* (**b**) *bladelet core from surface, cryptocrystalline silicate;* (**c**) *'thumbnail' scraper from Level 1 in Unit 1, hornfels;* (**d**) *large point from surface, hornfels;* (**e**) *notched piece from surface, banded ironstone;* (**f**) *'steep' scraper from Level 4 in Unit 3, hornfels.*

tures above 500° C (Weiner 2010; Shaw 2022). In addition, the bands at 2014 and 700 cm^{-1} are consistent with the presence of β-tricalcium phosphate, a phase that forms around 900°C (Etok *et al*. 2007). Except for the two calcined fragments mentioned above, bones were not recovered *in situ* in the excavation trenches. One cluster was found eroding out of the donga section about 1 m south of Unit 1. The bones in this assemblage are diagenetically altered, as shown by the infrared splitting factor of carbonate hydroxyapatite ranging between 3 and 4, and by the absence of collagen (Asscher *et al*. 2011).

MICROMORPHOLOGY

The analysis of micromorphology thin sections shows that SU1 is characterised by a channel microstructure, whereby pores in the form of channels occur ubiquitously throughout the sample, which is otherwise massive and does not exhibit sedimentary structures. The coarse fraction is dominated by very fine sand and silt that comprise sub-angular grains of quartz and feldspars. Sub-rounded grains of magnetite in the very fine sand size class are also present, as well as rare fragments of Ecca shale. The fine fraction includes brown clay, especially coating grains, and this layout produced a grano-striated birefringence fabric, in which clay domains appear oriented around sand and silt grains when observed in cross-polarised light (Fig. 9A). Pedofeatures include pore infillings of coarse grains caused by roots and microfauna, as shown by the occurrence of fragments of plant tissue (Fig. 9B), clay intercalations (Fig. 9C–D), and mite droppings (Fig. 9E). The boundary between SU1 and SU2 appears wavy and sharp (Supplementary Fig. 6). SU2 shares the same microstructure and composition as SU1, although the proportion of channels is lower, and the fine fraction is almost absent and concentrated around grains. The coarse fraction of SU2 includes sub-rounded, medium sand grains, and rounded pellets of clay in the very fine sand class (Fig. 9F). Pedofeatures are limited to coarse infillings.

PHYTOLITHS

Phytoliths were observed in all of the samples collected from the excavation trench (DMV-PHYT1-6), whereas the red palaeosol (DMV-PHYT7) was completely devoid of phytoliths. Level 1 produced the largest amount with more than one million phytoliths per gram of sediment; quantities decrease with increasing depth (Fig. 10). The overall preservation of phytoliths is poor, with evidence of extensive surface pitting and large amounts of weathered morphotypes. In fact, recognisable morphotypes include only those from motor cells (BLOCKY, BULLIFORM FLABELLATE), epidermal appendages (ACUTE BULBOSUS), and short cells of grasses (SADDLE, BILOBATE, RONDEL), which are more resistant to chemical dissolution (Cabanes *et al*. 2011) (Fig. 11). No morphotypes of dicotyledonous plants were observed. The proportions of grass short cells indicate the predominance of C_4 grasses (Chloridoideae-SADDLE, and Panicoideae-BILOBATE) in Levels 1–3, which account for more than 60% of the short cell assemblage. On the contrary, C_3 grasses (Pooideae-RONDEL) are the main component of Levels 4–5 (Fig. 10). The phytolith yield of Level 6 was too low to produce meaningful numbers.

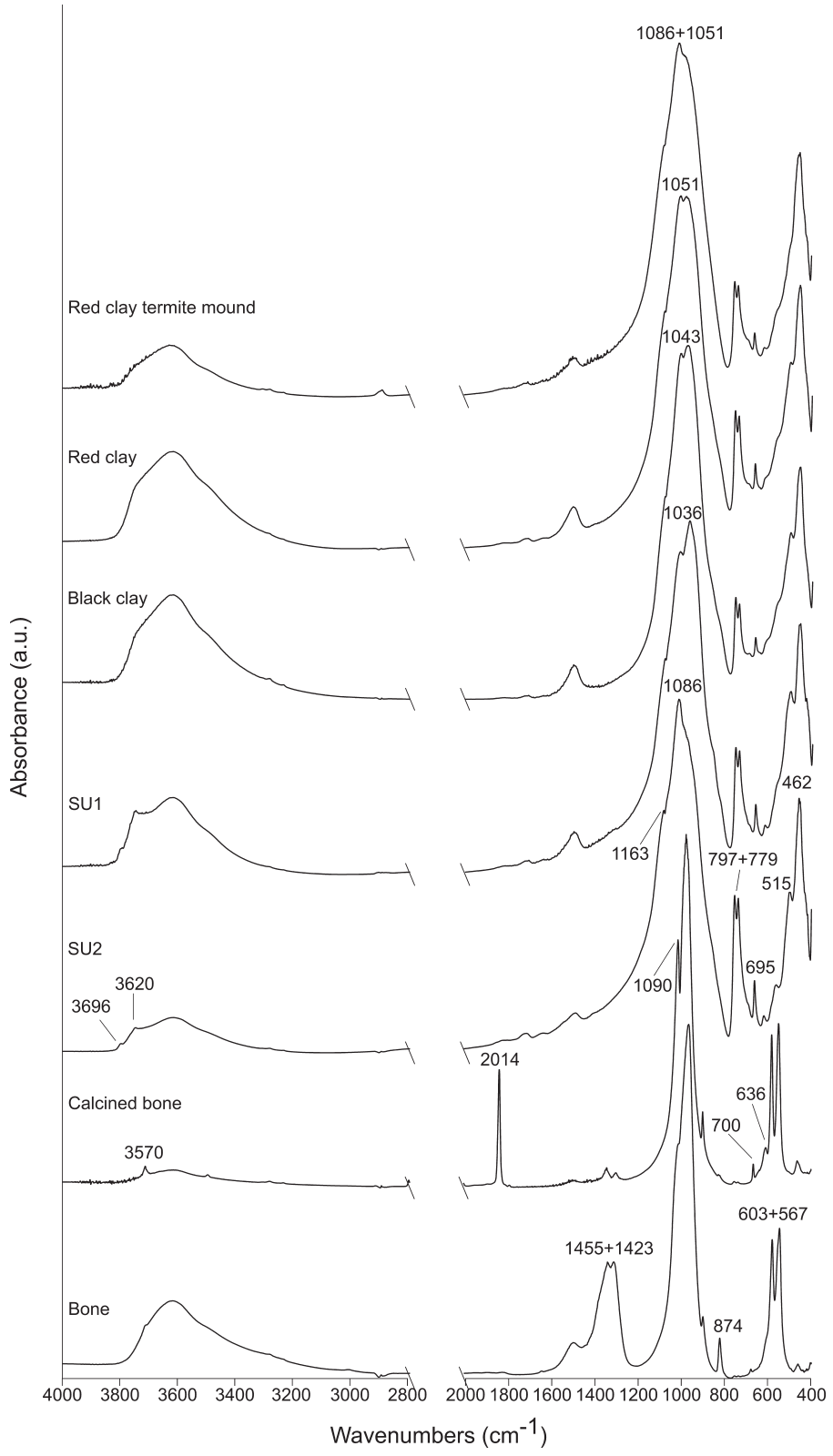

FIG. 8. *FTIR spectra of sediments and bones from Damvlei, including the Florisbad clay reference from the burned termite mound (a.u. = arbitrary units).*

FAUNA

The available fauna from the two Damvlei collections numbers 119 specimens; 41 were collected in 1995/96 and a further 78 during the 2019/21 seasons. Only two bone fragments were recovered from the 2019/21 excavations, and both represent very small, unidentified mammalian shaft fragments.

The other remains described here were found eroding from sections, or lying in adjacent gullies, and they exhibit exfoliation of the cortical tissue probably resulting from their exposure to the elements on the donga surface. As illustrated in Fig. 12, there are marked differences in skeletal element representation between the 1995/96 and 2019/21 collections. The majority of pieces from the earlier 1995/96 collection represent isolated teeth or teeth in jaws, followed by postcranial elements, all of which could be identified to skeletal part and/or body size if not genus. No unidentified bone fragments were present in this collection. The opposite was true for the 2019/21 collection, where unidentified bone fragments predominate,

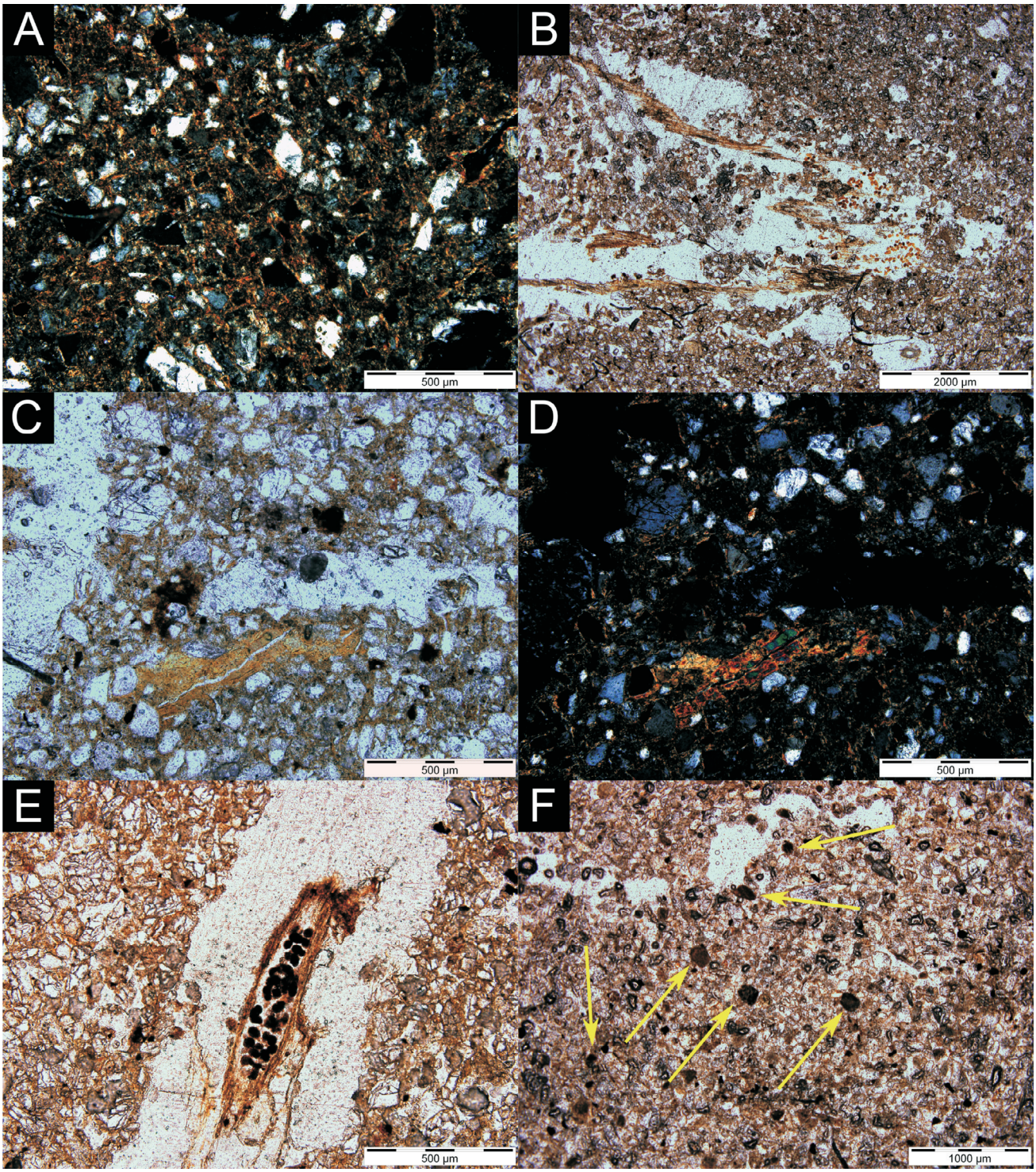

FIG. 9. *Photomicrographs of thin sections from Damvlei:* (**A**) *SU1, grano-striated birefringence fabric (cross-polarised light);* (**B**) *SU1, root channel partially infilled by sand, showing remains of plant tissue;* (**C**) *SU1, clay intercalation;* (**D**) *same as C, cross-polarised light;* (**E**) *SU1, mite droppings inside plant tissue in pore;* (**F**) *SU2, clay pellets (arrows).*

followed by isolated teeth. All faunal material that was visible at the time of the 2019/21 excavations was collected, suggesting that the earlier field collection may have been selective and only identifiable elements were taken. Together, these two collections reflect the faunal richness of this find locality. As can be seen in Table 4, the 1995/96 collection yielded remains of 12 different species, while the 2019/21 sample comprises remains of seven species. The difference may be attributed to the number of skeletal elements that could be identified in each collection; all 41 finds from the earlier collection were diagnostic *versus* only 17 from the 2019/21 sample. In fact, the more recent collection appears to represent a sub-sample of the earlier one, with all the species represented occurring in the larger 1995/96 assemblage.

Notably, both assemblages lack remains of birds, reptiles, fish, and microfauna. With one exception, an ulna of a lion (*Panthera leo*), the assemblage consists entirely of remains of herbivores (Fig. 13), with remains of equids the most common, represented by two species, the extinct Cape zebra, *Equus capensis* (Supplementary Fig. 7), and the locally extirpated plains zebra, *Equus quagga* (Groves & Bell 2004). A range of other grazers are represented including a bovine – the giant

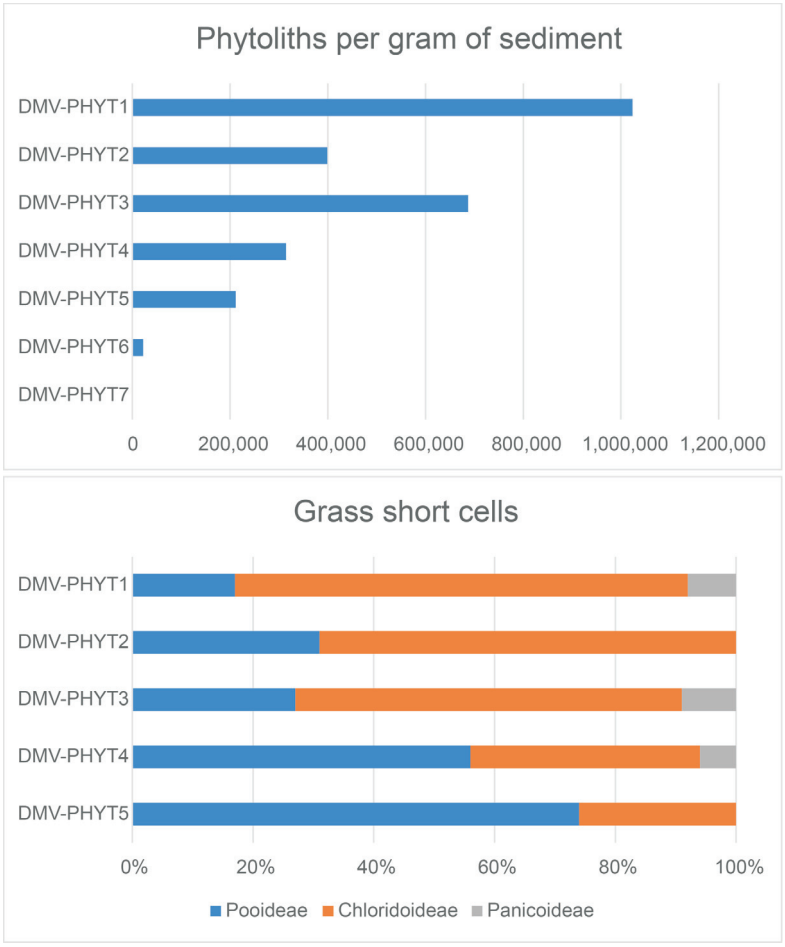

FIG. 10. *Phytolith concentrations* (**top**) *and proportions of grass short cells* (**bottom**) *in the Damvlei sediment samples, in stratigraphic order. Sample numbers correspond to excavation levels except for number 7, which is the red palaeosol.*

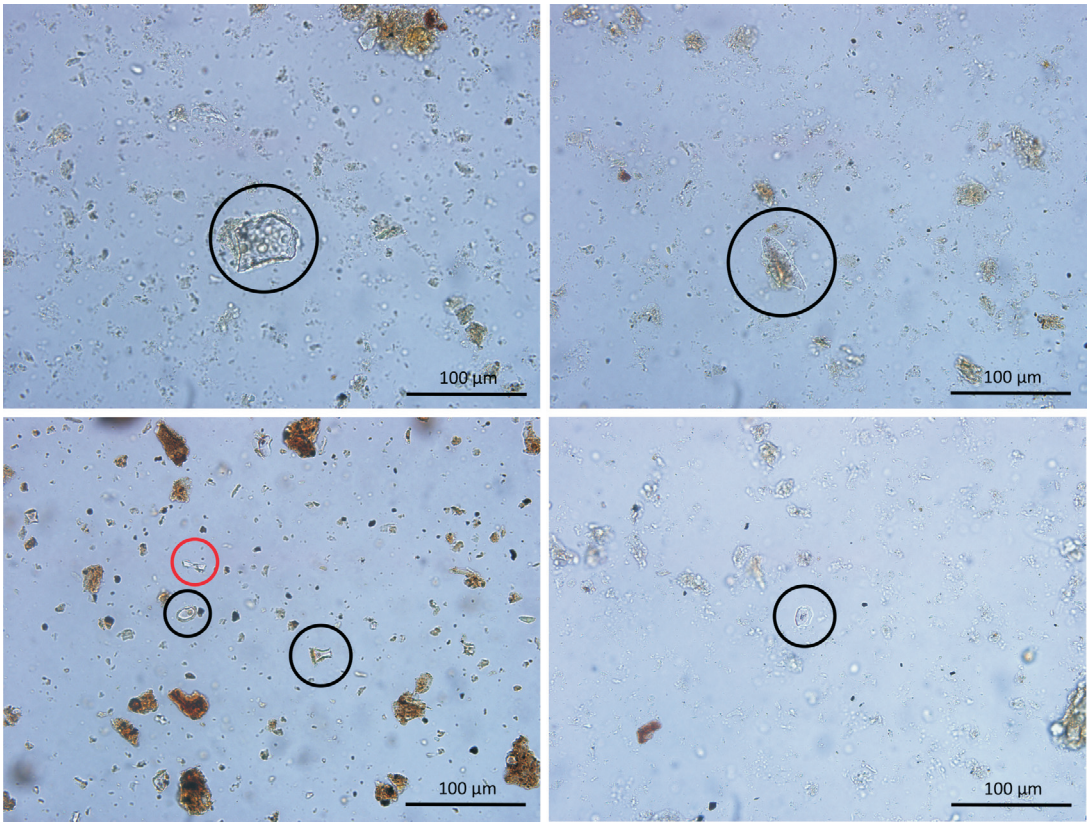

FIG. 11. *Phytolith morphotypes identified at Damvlei (marked by circles).* **Top left**: *BULLIFORM FLABELLATE showing evidence of pitting.* **Top right**: *ACUTE BULBOSUS showing evidence of pitting.* **Bottom left**: *Bilobate (red circle) and RONDEL (black circles) short cells.* **Bottom right**: *SADDLE short cell.*

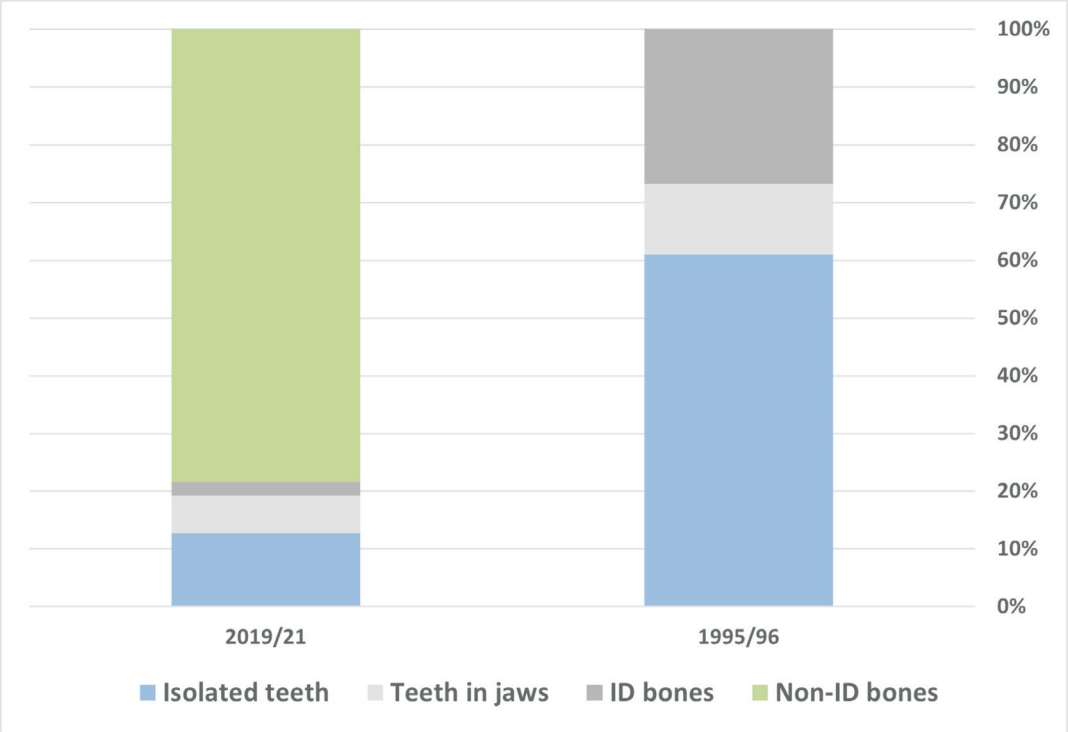

FIG. 12. *Breakdown of skeletal elements in the two samples from Damvlei.*

African buffalo, *Syncerus [Pelorovis] antiquus*; small-sized antelopes such as duiker (*Sylvicapra grimmia*), steenbok (*Raphicerus campestris*), and the greater kudu (*Tragelaphus strepsiceros*) – a browser (Supplementary Fig. 8). Alcelaphines present include both hartebeest (*Alcelaphus buselaphus*) (Supplementary Fig. 9) and the extinct *Megalotragus priscus*. The remains of the black wildebeest, *Connochaetes gnou* (also known as the white-tailed gnu) were distinguished from those of the blue wildebeest (*Connochaetes taurinus*, Supplementary Fig. 10) on the basis of size – the blue wildebeest being larger (Fig. 14). Damvlei lies at the very southern extent of the current biogeographical range of the blue wildebeest – the Orange River – and our finds may serve as corroboration that this was its range in the past. In terms of second molar tooth dimensions, the Damvlei wildebeest and hartebeest specimens overlap the size range of those from the MSA site of Florisbad, though Damvlei sample sizes are extremely small.

TABLE 4. *Damvlei species list (NISP: number of identified specimens). Bovid size classes based on Brain (1974).*

Species	Extinct	1995/96 NISP	2019/2 NISP
Alcelaphines			
Large Alcelaphine (*Megalotragus priscus*)	Yes	5	1
Hartebeest (*Alcelaphus buselaphus*)		1	
Alcelaphus sp.			1
Wildebeest *cf.* blue (*Connochaetes* cf. *taurinus*)		2	4
Antelopes and bovids			
Duiker (*Sylvicapra grimmia*)		1	1
Springbok sp. (*Antidorcas* sp.)		5	
Greater kudu (*Tragelaphus strepsiceros*)		1	
Steenbok (*Raphicerus campestris*)		1	
Giant African buffalo (*Syncerus antiquus*)	Yes	2	
Bovid size class IV		1	
Bovid Size class III		2	
Bovid size class II–III		1	
Bovid undetermined		5	
Suids			
Warthog *cf.* common warthog (*Phacochoerus* cf. *aethiopicus*)		1	1
Equids			
Plains zebra *(Equus quagga*)		7	2
Giant Cape zebra *(Equus capensis*)	Yes	5	5
Equid sp.			2
Carnivores			
Lion (*Panthera leo*)		1	
Total		41	17

OSL DATING

The distributions of natural equivalent doses are dispersed (overdispersions of 111 ± 11 and 86 ± 8% respectively for DMV1 and DMV2, Table 5). While issues with poor bleaching cannot completely be ruled out, the dispersion was mainly attributed to bioturbation (microfauna and plant roots) that were already observed in the field and could not be fully avoided during sampling. It is also unlikely, even though we did not measure it, that the dispersion be due to the microdosimetric effect, as it is not expected with this type of sediment. Graphical representation and application of the Finite Mixture Model (Roberts *et al*. 2000) with variable sigma_b values, suggests at least three to four populations, close to 0, 10, and 25 Gy, and between 50–100 Gy for the two samples. However, determining an age from the Finite Mixture Model would be highly speculative, first because there is no clearly dominating population, and second because the significance of the mean dose rate in that case is problematic. Consequently, a

TABLE 5. *Data related to the natural equivalent dose measurements. N: number of measured grains; n1: number of grains that pass the sensitivity and recuperation criteria; n2: number of grains that pass the* D_0 *threshold criteria. OD = overdispersion.*

Sample	N	n1	n2	D_0 (Gy)	OD (%)
DMV1	800	89	62	40	111 ± 11
DMV2	1500	187	90	40	86 ± 8

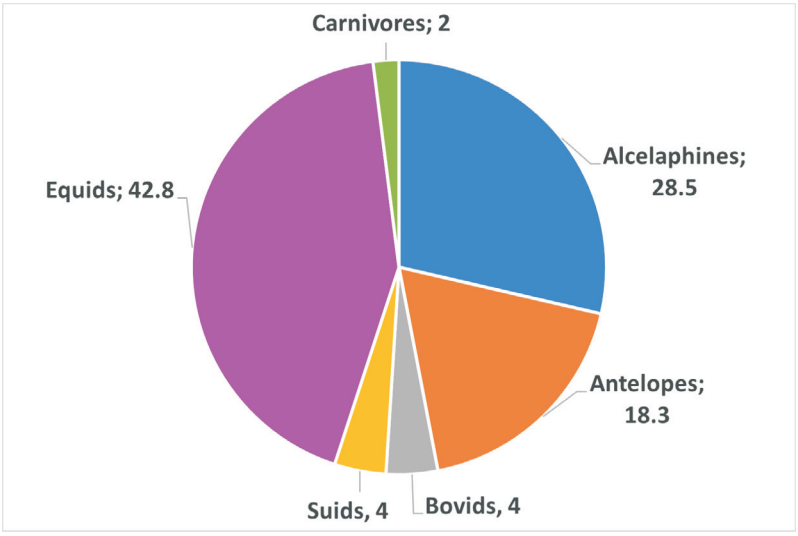

FIG. 13. *Representation of faunal families at Damvlei (%).*

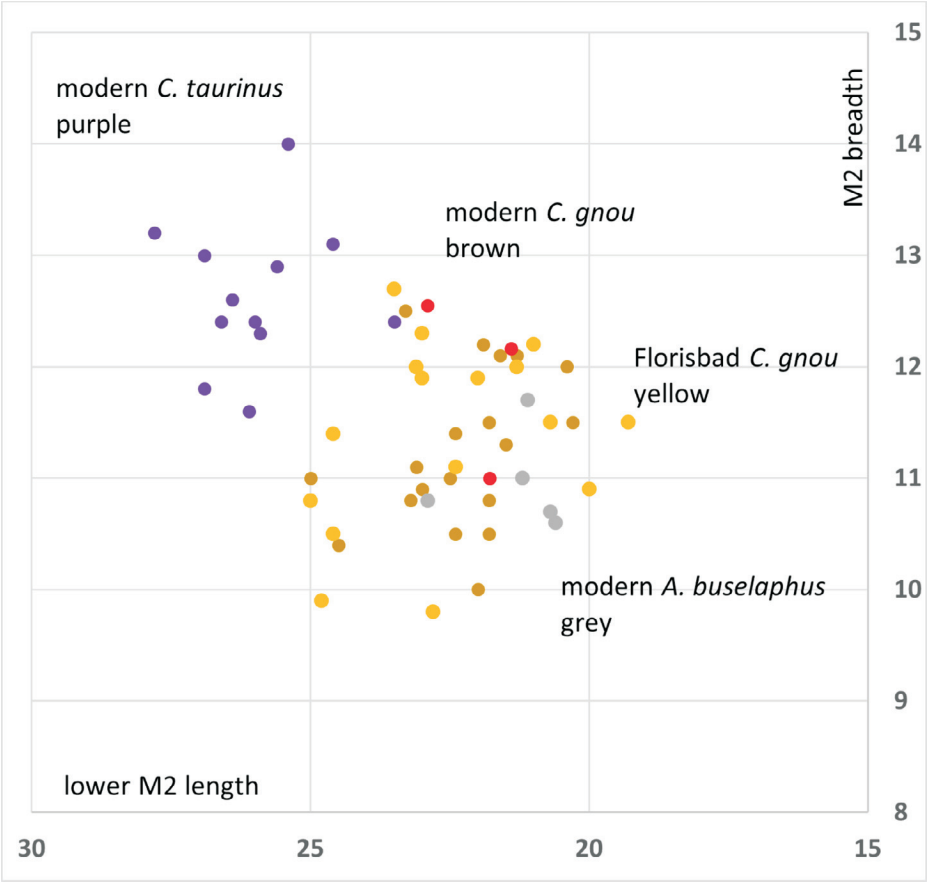

FIG. 14. *Measurements of Alcelaphine lower second molar teeth from Damvlei (red dots) compared to three modern alcelaphines and Florisbad MSA specimens. Note that three hartebeest specimens from Damvlei fall in the black hartebeest range while another specimen, identified as hartebeest, falls within the range of this species. Measurements of individual teeth were taken at the occlusal surface and are given in mm. All measurements (except for Damvlei) were taken from Brink (2005: table 24).*

maximum dose estimate was calculated for DMV2, for which more grains have been measured, from the highest component. This was estimated at 68 ± 4 Gy (Fig. 15). The estimated dose rate for DMV2 is 2.55 ± 0.18 Gy/ka (Table 6). As mentioned above, its significance for an age calculation is disputable, because of the suspicion of strong bioturbation. Nonetheless, it is in the (high) range of what has been obtained at the nearby site of Lovedale for less disturbed samples (Wroth *et al*. 2022), and for that reason it can be used to obtain the maximum age estimate of 27 ± 3 ka, which falls within MIS 2.

RADIOCARBON DATING

Sediments for radiocarbon dating were tested for mineral composition, showing mainly quartz and clay minerals (Fig. 8). The carbonate content ranged between 5.5% and 8.4%. The radiocarbon age determinations obtained from the TOC of Unit 1 sediments span the past ~3400 years, with the topmost sample (5 cm below surface) dated to the 1950s based on the 'bomb peak' in the calibration curve, and the portion of stratigraphy between 25 and 55 cm below surface ranging from ~1400 BC to ~1450 AD (Table 7).

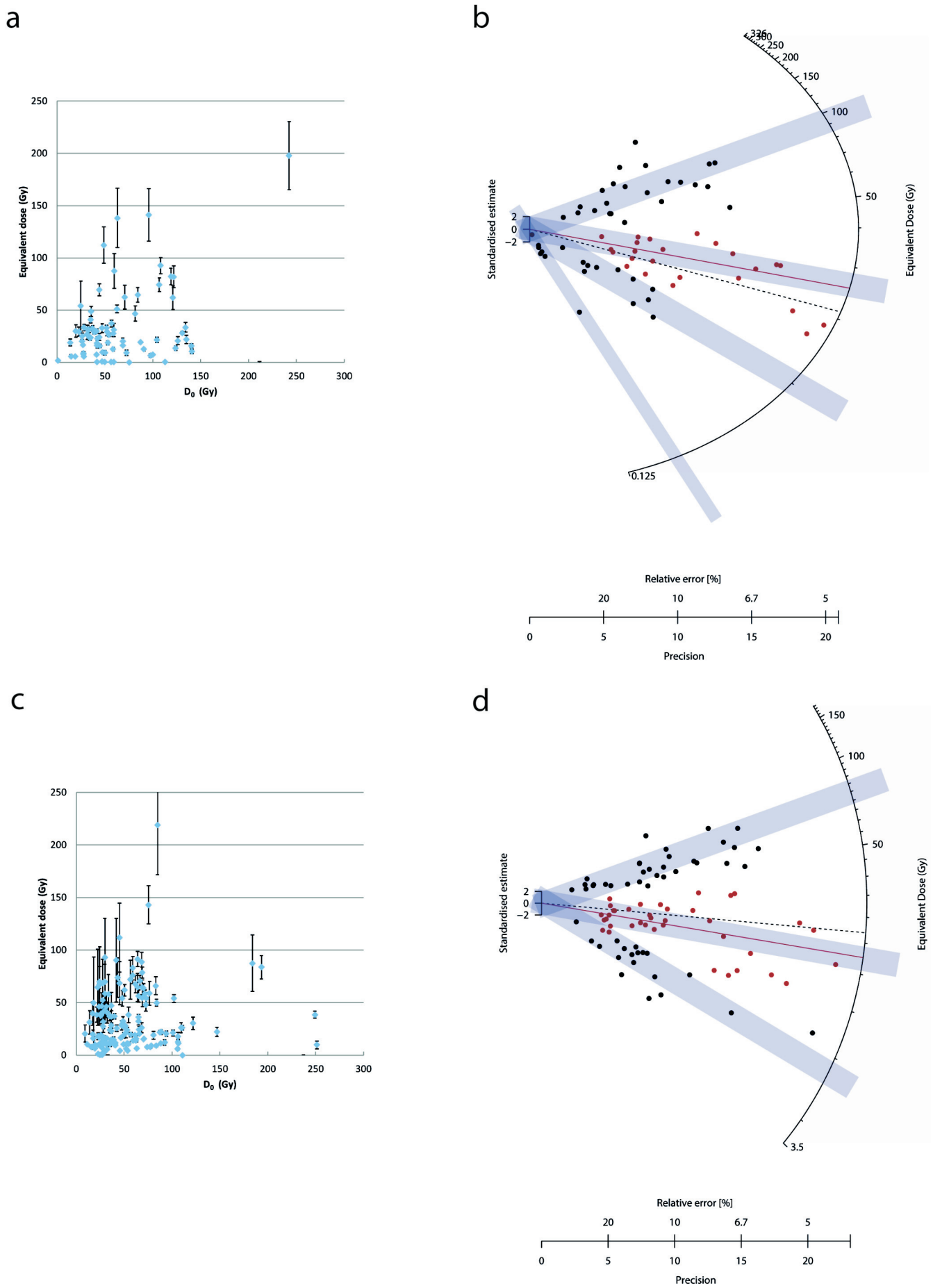

FIG. 15. *Plots of data for the equivalent dose* (D_e) *measurements;* (**a**) D_e *as a function of* D_0 *for DMV1;* (**b**) *radial plot for the* D_e *values of DMV1, for* $D_0 > 40$ *Gy. The grey bars show the components that are suggested by the Finite Mixture Model for sigma_b = 0.3;* (**c**) *and* (**d**) *same as A and B, respectively, for DMV2.*

TABLE 6. *Dose rate data based on a past water content of 30 ± 8%, expressed in Gy/ka.*

Sample	Cosmic dose rate	Gamma dose rate	Beta dose rate	Total
DMV1	0.24 ± 0.02	0.84 ± 0.07	1.18 ± 0.14	2.26 ± 0.16
DMV2	0.24 ± 0.02	0.86 ± 0.07	1.46 ± 0.16	2.55 ± 0.18

DISCUSSION

The micro-geoarchaeological approach deployed in this research permitted a robust reconstruction of the site formation processes. Micromorphology and FTIR have already been used to provide greater insights into sediments and fossils of Early and Middle Pleistocene sites in the Free State (Toffolo *et al*. 2015, 2019; Toffolo *et al*. 2017; Scott *et al*. 2019), and recently have been applied to LSA contexts in the Northern Cape (Rhodes *et al*. 2022). In particular, the reference FTIR spectra for heat-altered sediments can be used for other sites in the region to estimate the temperature of burning of clay minerals.

The massive microstructure interrupted by channels observed in the micromorphology thin sections indicates that SU1 formed as a result of low-energy, overbank sedimentation of the Modder, a process unlikely to displace artefacts lying on the surface and rather favourable to the preservation of primary depositional contexts. This process took place several times, since the occurrence of artefacts at different depths can be interpreted as a series of exposed land surfaces. Given the current position of the Modder riverbed, it would appear that human occupation took place close to the water, at least with regard to the Lockshoek artefacts from Levels 2–6. Level 5, which produced one of the highest lithic counts, yielded aggregates of burned sediment and two fragments of calcined bone, as shown with FTIR. While these components may be the result of human activities related to food processing, the absence of a combustion structure and the open-air nature of the site do not allow the exclusion of a wildfire or controlled veld fire as the cause for their presence (Gowlett *et al*. 2017). No other faunal remains were found *in situ*. Nevertheless, animal remains must have been a common occurrence at the site based on the abundance of bones on the donga floor and the fact that clusters were found eroding from bluffs, notably at ~60 cm depth right to the south of Unit 1. The depositional environment changed in SU2, which is an aeolian sand rich in windblown clay pellets (Goldberg *et al*. 2015; Toffolo *et al*. 2017). Here, too, it is considered that artefacts are in a primary depositional context, given that wind alone cannot displace lithics. Both SU1 and SU2 have been affected by post-depositional processes, especially the disruptive effect of plant roots and microfauna, which produced large channels that favoured coarse illuviation and subsequent displacement of quartz grains. In turn, this process hampered dating of DMV1 by OSL due to extensive mixing, and allowed only a maximum age for DMV2. Similarly, post-depositional circulation of water, represented by clay intercalations and coarse infillings, promoted the diffusion of modern organic carbon, which produced younger radiocarbon age determinations for all dated levels, which are not consistent with the occurrence of Wilton and Lockshoek artefacts. In fact, the Damvlei radiocarbon dates, covering the last ~3400 years (Table 7), are significantly younger compared to the age range of the Oakhurst technocomplex in other parts of the Free State and South Africa, which is ~12–8 ka (Wadley 1993; Mitchell 2000, 2016).

Faunal remains and phytoliths provided more detailed information for the reconstruction of past environments at Damvlei. Given the predominance of grazers, especially equids, the site was likely located in an open grassland habitat. The range of species represented is typical of the Florisian Land Mammal Age, currently also known as the late Naivashan (Van Couvering & Delson 2020), and common in other Florisian assemblages found in the southern African interior including the Riet and Modder Rivers (Brink 1987, 1988; Brink *et al*. 1999; Brink 2005). The upper limit of the Florisian falls around 600 000 years ago, while the lower limit is the end of the Pleistocene/early Holocene (Klein 1984; Brink 2016). The Florisian fossil assemblages typically include five extinct grazers: Bond's springbok, *Antidorcas bondi*; a species of tsessebe, *Damaliscus niro*; *M. priscus*; *E. capensis*; and *S. antiquus* (Hendey 1974; Klein 1984; Brink 1987; Brink & Lee-Thorp 1992; Brink 2005). Also present are modern forms such as the black wildebeest. The absence of small-sized faunal taxa is also considered typical of Florisian fossil assemblages (Brink 2005). The Damvlei assemblage contains several typical Florisian species – *M. priscus*, *E. capensis*, *E. quagga*, and *S. antiquus*. Notably absent in the Damvlei assemblage are remains of species that are associated with marshy and aquatic conditions, such as lechwe (*Kobus leche*), waterbuck (*Kobus ellipsiprymnus*), and hippopotamus (*Hippopotamus amphibius*), which occur in other Florisian sites, such as at Florisbad (Brink 1987, 1988) and the Riet River gravels (Berger & Brink 1996). Also missing at Damvlei are remains of Bond's springbok, a keystone species of the Florisian that went extinct in the early Holocene (~10–8 ka) (Ecker & Lee-Thorp 2018). In contrast to the common springbok (*Antidorcas marsupialis*), which is a flexible mixed feeder that can tolerate arid habitats, *A. bondi* was a small-bodied specialised grazer that consumed C_4 grasses, and whose presence reflects the high quality of the grasslands at this time. However, a dental microwear study (Sewell *et al*. 2019), suggests that *A. bondi* may have had a mixed diet that was more similar to that of *A. marsupialis*. The latter species is present at Damvlei. Rossouw (2006) noted that the absence of typical Florisian taxa does not necessarily reflect their past availability in the region. He suggested that selective taphonomic factors may be responsible for their absence. However, it is unlikely that selective diagenesis is responsible for the species range found at Damvlei given the similar size of the herbivores that are represented and those that are missing. Thus, it is more feasible that other factors are at play, for example sample size, with remains of species that are somewhat rare in the landscape, underrepresented in small fossil assemblages (Grayson 1984; Lyman 2012). However, it is more likely that the fossil

TABLE 7. *Radiocarbon dating results (pMC: percentage of Modern Carbon). The C% refers to the measured carbon extracted calculated on the mass of sediment after 1 M HCl, therefore after removal of the carbonate fraction.*

Sample no.	Context	Carbonate %	C%	pMC	Age BP	Age BC–AD (1σ)
RTD 11805	Unit 1 Level 1	5.6	0.39	102.722 ± 0.257	–215 ± 20	1953–1957 AD
RTD 11806	Unit 1 Level 3	5.5	0.09	93.601 ± 0.254	531 ± 21	1420–1442 AD
RTD 11807	Unit 1 Level 6	8.4	0.13	67.892 ± 0.162	3110 ± 19	1396–1367 BC (20.3%) 1358–1290 BC (48%)

spectrum reflects the palaeoenvironmental conditions of the late Florisian. Indeed, the late Pleistocene/early Holocene in the interior of southern Africa was characterised by comparatively more arid conditions than in the preceding Middle Pleistocene, for instance at Erfkroon (Lyons *et al*. 2014), although more C_3 plants were available in the local vegetation up to ~7 ka in comparison to the subsequent mid- and late Holocene environments (Ecker *et al*. 2018; Lukich & Ecker 2022). This scenario is in agreement with the evidence from phytoliths, which clearly shows a predominance of C_3 grasses in the Lockshoek levels (dated to ~12–8 ka in South Africa), whereas drier conditions, represented by the Chloridoideae morphotypes produced by C_4 grasses, were established in the levels featuring Wilton assemblages, the latter dated to the middle and late Holocene in South Africa (Mitchell 2000, 2016). Although Brink (2005) noted that in some parts of the interior a wetland component endured until the end of the Florisian, increasing aridity would be the most parsimonious explanation for the lack of water-adapted taxa at Damvlei, despite the proximity of the site to the Modder River. If the chronological explanation is correct, then Damvlei is indeed a representative of the late Florisian and may represent one of the last appearances of *E. capensis*, *M. priscus*, and *S. antiquus* (Faith 2014; Ecker & Lee-Thorp 2018), since this Land Mammal Age was associated with the extinction of a wide spectrum of herbivores.

Evidence from sediments, fauna, and phytoliths showed that Damvlei was an open grassland environment characterised by relatively wetter conditions in the early Holocene and drier conditions in the middle and late Holocene. In this context, human occupation took place close to the riverbank, most likely as a series of short-lived visits taking advantage of exposed surfaces near the water. The occurrence of artefacts made of banded ironstone, which is an allochtonous rock whose closest source is located in the Kuruman Hills, ~230 km to the north-west, lends support to the interpretation that these groups had extensive social networks, consistent with the widespread occurrence of Oakhurst and Wilton assemblages across the subcontinent (Sealy 2016). The tempo of these occupations can only be framed at its older end using OSL, and the chronological sequence of the archaeological levels relies mostly on the age range of the Oakhurst and Wilton technocomplexes. The lowermost excavated level in SU1 produced a maximum age of 27 ± 3 ka, which predates the overlying Lockshoek and Wilton artefacts, dated to the Holocene in other parts of South Africa (Wadley 1993; Mitchell 2000, 2016), and all of the lithics and fauna from the donga floor and bluffs, which were collected in places located at a higher elevation compared to DMV2 and the red palaeosol. The latter, based on the DMV2 date, could be contemporary with an extensive red palaeosol described 11 km downstream at Erfkroon, and dated to ~33 ka (Lyons *et al*. 2014; Bousman, Brink, *et al*. 2023). Taking into account the possibility that part of the surface assemblage might belong to the earlier Robberg technocomplex, which needs to remain open until a detailed examination of the full lithic assemblage is available, it appears that the Damvlei data do not support a scenario of permanent human presence in the interior grasslands during the terminal Pleistocene, and especially during the LGM, and that occupation before the Holocene might have been only ephemeral and limited to some of the Florisian wetlands along rivers, such as the Modder (Brink 2016; Mitchell 2017; Bousman, Brink, *et al*. 2023), whereas permanent presence was confined to the better-watered highlands towards the east (Stewart *et al*. 2016; Stewart & Mitchell 2018).

CONCLUSIONS

Excavations at the Damvlei donga unearthed a series of LSA occupations on the bank of the Modder River, which collectively span the Holocene, although sediments and faunal remains go back at least to the terminal Pleistocene. The study of sediments and fossils highlighted the importance of analyses at the microscale in assessing the integrity of materials for absolute dating, especially with regard to bioturbation and the post-depositional displacement of carbon and sand grains, and in determining the primary depositional context of the artefacts. In addition, it was possible to detect heat-altered components related to fire despite the absence of a combustion structure. For these reasons, we advocate the application of a micro-geoarchaeological approach to better understand formation processes at open-air sites. Results emphasise the need for a more extensive investigation of LSA occurrences in the grasslands of the Highveld, including geochronology, in order to frame the timing of human presence in the central interior, especially in relation to the Robberg technocomplex, which is currently represented only in undated contexts at Erfkroon.

ACKNOWLEDGEMENTS

This work is dedicated to the memory of James Simpson Brink (1957–2019), our friend and colleague. Fieldwork was carried out under the auspices of the Florisbad Quaternary Research Department, National Museum Bloemfontein. The excavation permit was issued to Lloyd Rossouw and Michael Toffolo by the South African Heritage Resources Agency (permit ID 2862). Research was funded by a grant from the Deutsche Forschungsgemeinschaft to Christopher Miller (grant no. MI 1748/4-1), and by the National Museum Bloemfontein. Michael Toffolo was supported by a grant from IdEx Bordeaux (grant no. ANR-10-IDEX-03-02), and by the grant RYC2021-030917-I funded by the MCIN/AEI/10.13039/5011000 11033 and by the "European Union NextGenerationEU/PRTR". We would like to thank the following people: Frans Du Toit, owner of the Strydomspan farm, for granting permission to conduct fieldwork on his property and for his continued interest in the prehistory of the Free State and unwavering support of our work; the late Isaac Thapo, Jacob Maine, Abel Dichakane, Peter Mdala, Johannes Motshabi, Moses Mahloko, and Kristen Wroth for their assistance during fieldwork; Tria Oersen and Jaco Smith for facilitating our stay at the Florisbad Research Station during fieldwork seasons; Sharon Holt for helping us sort through collections at Florisbad; Cornie van Huyssteen for lending us a petrographic microscope during excavations. We are grateful to Carlos Sáiz Dominguez for preparing thin sections. We thank the editor and reviewers for their comments which improved the manuscript.

REFERENCES

Asscher, Y., Regev, L., Weiner, S. & Boaretto, E. 2011. Atomic disorder in fossil tooth and bone mineral: an FTIR study using the grinding curve method. *ArcheoSciences* 35: 135–141.

Barker, C.H. 2011. Utilising published data for DTM construction and drainage basin delineation in the Modder River catchment, Free State, South Africa. *South African Geographical Journal* 93(1): 89–103.

Behrensmeyer, A.K. 1978. Taphonomic and ecologic information from bone weathering. *Paleobiology* 4(2): 150–162.

Berger, L.R. & Brink, J. 1996. Late Middle Pleistocene fossils, including a human patella, from the Riet River gravels, Free State, South Africa. *South African Journal of Science* 92(6): 277–278.

Berna, F., Behar, A., Shahack-Gross, R., Berg, J., Boaretto, E., Gilboa, A., Sharon, I., Shalev, S., Shilstein, S., Yahalom-Mack, N., Zorn, J.R. & Weiner, S. 2007. Sediments exposed to high temperatures: reconstructing pyrotechnological processes in Late Bronze and Iron Age strata at Tel Dor (Israel). *Journal of Archaeological Science* 34(3): 358–373.

Bøtter-Jensen, L., Bulur, E., Duller, G.A.T. & Murray, A.S. 2000. Advances in luminescence instrument systems. *Radiation Measurements* 32(5): 523–528.

Bousman, B., Codron, D., Gowlett, J., Herries, A.I.R., Rossouw, L. & Toffolo, M. 2023. Cornelia-Uitzoek, South Africa. In: Beyin, A., Wright, D.K., Wilkins, J. & Olszewski, D.I. (eds) *Handbook of Pleistocene Archaeology of Africa: Hominin Behavior, Geography, and Chronology*: 1327–1347. Cham: Springer International Publishing.

Bousman, B., Brink, J., Rossouw, L., Bateman, M., Morris, S., Meier, H., Bronk Ramsey, C., Trower, G., Herries, A.I.R., Ringstaff, C., Thornton-Barnett, S. & Dworkin, S. 2023. Erfkroon, South Africa. In: Beyin, A., Wright, D.K., Wilkins, J. & Olszewski, D.I. (eds) *Handbook of Pleistocene Archaeology of Africa: Hominin Behavior, Geography, and Chronology*: 1431–1450. Cham: Springer International Publishing.

Bousman, C.B. & Brink, J.S. 2018. The emergence, spread and termination of the Early Later Stone Age event in South Africa and southern Namibia. *Quaternary International* 495: 116–135.

Brain, C.K. 1974. Some suggested procedures in the analysis of bone accumulations from southern African Quaternary sites. *Annals of the Transvaal Museum* 29(1): 1–8.

Brink, J.S. 1987. The archaeozoology of Florisbad, Orange Free State. *Memoirs van die Nasionale Museum*, *Bloemfontein* 24: 1–151.

Brink, J.S. 1988. The taphonomy and palaeoecology of the Florisbad spring fauna. *Palaeoecology of Africa and the Surrounding Islands* 19: 169–179.

Brink, J.S. 2004. The taphonomy of an Early/Middle Pleistocene hyaena burrow at Cornelia-Uitzoek, South Africa. *Revue de Paléobiologie* 23: 731–740.

Brink, J.S. 2005. The evolution of the black wildebeest, *Connochaetes gnou*, and modern large mammal faunas in central southern Africa. Unpublished PhD thesis. Stellenbosch: Stellenbosch University.

Brink, J.S. 2016. Faunal evidence for a mid- and late Quaternary environmental change in southern Africa. In: Knight, J. & Grab, S.W. (eds) *Quaternary Environmental Change in Southern Africa: Physical and Human Dimensions*: 284–305. Cambridge: Cambridge University Press.

Brink, J.S. & Lee-Thorp, J.A. 1992. The feeding niche of an extinct springbok, *Antidorcas bondi* (Antelopini, Bovidae), and its palaeoenvironmental meaning. *South African Journal of Science* 88: 227–229.

Brink, J.S. & Rossouw, L. 2000. New trial excavations at the Cornelia-Uitzoek type locality. *Navorsinge van die Nasionale Museum Bloemfontein* 16: 141–156.

Brink, J.S. & Henderson, Z.L. 2001. A high-resolution Last Interglacial MSA horizon at Florisbad in the context of other open-air occurrences in the central interior of southern Africa: an interim statement. In: Conard, N.J. (ed.) *Settlement Dynamics of the Middle Paleolithic and Middle Stone Age*: 1–20. Tübingen: Kerns Verlag.

Brink, J.S., Berger, L.R. & Churchill, S.E. 1999. Mammalian fossils from erosional gullies (dongas) in the Doring River drainage, central Free State, South Africa. In: Berger, C., Manhart, H., Peters, J. & Schibler, J. (eds) *Historia animalium ex ossibus: Beiträge zur Paläoanatomie, Archäologie, Ägyptologie, Ethnologie und Geschichte der Tiermedizin: Festschrift für Angela von den Driesch*: 79–90. Rahden/Westfalen: Verlag Marie Leidorf.

Brink, J.S., Bousman, C.B. & Grün, R. 2016. A reconstruction of the skull of *Megalotragus priscus* (Broom, 1909), based on a find from Erfkroon, Modder River, South Africa, with notes on the chronology and biogeography of the species. *Palaeoecology of Africa* 33: 71–94.

Brink, J.S., Herries, A.I.R., Moggi-Cecchi, J., Gowlett, J.A.J., Bousman, C.B., Hancox, J.P., Grün, R., Eisenmann, V., Adams, J.W. & Rossouw, L. 2012. First hominine remains from a ~1.0 million year old bone bed at Cornelia-Uitzoek, Free State Province, South Africa. *Journal of Human Evolution* 63: 527–535.

Bronk Ramsey, C. 2009. Bayesian analysis of radiocarbon dates. *Radiocarbon* 51(1): 337–360.

Cabanes, D., Weiner, S. & Shahack-Gross, R. 2011. Stability of phytoliths in the archaeological record: a dissolution study of modern and fossil phytoliths. *Journal of Archaeological Science* 38(9): 2480–2490.

Churchill, S.E., Brink, J.S., Berger, L.R., Hutchinson, R.A., Rossouw, L., Stynder, D., Hancox, P.J., Brandt, D., Woodborne, S., Loock, J.C., Scott, L. & Ungar, P. 2000. Erfkroon: a new Florisian fossil locality from fluvial contexts in the western Free State, South Africa. *South African Journal of Science* 96: 161–163.

Clark, J.D. 1974. The stone artefacts from Cornelia, O.F.S., South Africa. *Memoirs van die Nasionale Museum*, *Bloemfontein* 9: 33–62.

Cooke, H.B.S. 1955. Some fossil mammals in the South African Museum collections. *Annals of the South African Museum* 42(3): 161–168.

De la Peña, P. & Witelson, D.M. 2020. 'Project Piedemonte': between the Maloti-Drakensberg and the Great Escarpment in the Eastern Cape Province, South Africa. *Antiquity* 94(376): e20.

De Ruiter, D.J., Churchill, S.E., Brophy, J.K. & Berger, L.R. 2011. Regional survey of Middle Stone Age fossil vertebrate deposits in the Virginia-Theunissen area of the Free State, South Africa. *Navorsinge van die Nasionale Museum Bloemfontein* 27(1): 1–20.

Dewar, G. & Stewart, B.A. 2017. Early maritime desert dwellers in Namaqualand, South Africa: a Holocene perspective on Pleistocene peopling. *The Journal of Island and Coastal Archaeology* 12(1): 44–64.

Duller, G.A.T. 2003. Distinguishing quartz and feldspar in single grain luminescence measurements. *Radiation Measurements* 37(2): 161–165.

Duller, G.A.T. 2015. The Analyst software package for luminescence data: overview and recent improvements. *Ancient TL* 33: 35–42.

Ecker, M. & Lee-Thorp, J.A. 2018. The dietary ecology of the extinct springbok *Antidorcas bondi*. *Quaternary International* 495: 136–143.

Ecker, M., Brink, J., Horwitz, L.K., Scott, L. & Lee-Thorp, J.A. 2018. A 12,000 year record of changes in herbivore niche separation and palaeoclimate (Wonderwerk Cave, South Africa). *Quaternary Science Reviews* 180: 132–144.

Etok, S.E., Valsami-Jones, E., Wess, T.J., Hiller, J.C., Maxwell, C.A., Rogers, K.D., Manning, D.A.C., White, M.L., Lopez-Capel, E., Collins, M.J., Buckley, M., Penkman, K.E.H. & Woodgate, S.L. 2007. Structural and chemical changes of thermally treated bone apatite. *Journal of Materials Science* 42(23): 9807–9816.

Faith, J.T. 2014. Late Pleistocene and Holocene mammal extinctions on continental Africa. *Earth-Science Reviews* 128: 105–121.

Farmer, V.C. 1974. *The Infrared Spectra of Minerals*. London: Mineralogical Society.

Goldberg, P., Berna, F. & Chazan, M. 2015. Deposition and diagenesis in the Earlier Stone Age of Wonderwerk Cave, Excavation 1, South Africa. *African Archaeological Review* 32: 613–643.

Gowlett, J.A.J., Brink, J.S., Caris, A., Hoare, S. & Rucina, S.M. 2017. Evidence of burning from bushfires in southern and East Africa and its relevance to hominin evolution. *Current Anthropology* 58(S16): S206–S216.

Grayson, D.K. 1984. *Quantitative Zooarchaeology. Topics in the Analysis of Archaeological Faunas*. Orlando: Academic Press.

Groves, C.P. & Bell, C.H. 2004. New investigations on the taxonomy of the zebras genus *Equus*, subgenus *Hippotigris*. *Mammalian Biology* 69(3): 182–196.

Guérin, G., Mercier, N. & Adamiec, G. 2011. Dose-rate conversion factors: update. *Ancient TL* 29: 5–8.

Guérin, G., Mercier, N., Nathan, R., Adamiec, G. & Lefrais, Y. 2012. On the use of the infinite matrix assumption and associated concepts: a critical review. *Radiation Measurements* 47(9): 778–785.

Hallinan, E. 2021. Landscape-scale perspectives on Stone Age behavioural change from the Tankwa Karoo, South Africa. *Azania: Archaeological Research in Africa* 56(3): 304–343.

Hallinan, E. 2022. "A Survey of Surveys" revisited: current approaches to landscape and surface archaeology in southern Africa. *African Archaeological Review* 39(1): 79–111.

Hansen, V., Murray, A., Buylaert, J-P., Yeo, E-Y. & Thomsen, K. 2015. A new irradiated quartz for beta source calibration. *Radiation Measurements* 81: 123–127.

Hendey, Q.B. 1974. The Late Cenozoic Carnivora of the south-western Cape Province. *Annals of the South African Museum* 63: 1–369.

Hogg, A.G., Heaton, T.J., Hua, Q., Palmer, J.G., Turney, C.S.M., Southon, J., Bayliss, A., Blackwell, P.G., Boswijk, G., Bronk Ramsey, C., Pearson, C., Petchey, F., Reimer, P., Reimer, R. & Wacker, L. 2020. SHCal20 Southern Hemisphere Calibration, 0–55,000 Years cal BP. *Radiocarbon* 62(4): 759–778.

Katz, O., Cabanes, D., Weiner, S., Maeir, A.M., Boaretto, E. & Shahack-Gross, R. 2010. Rapid phytolith extraction for analysis of phytolith concentrations and assemblages during an excavation: an application at Tell es-Safi/Gath, Israel. *Journal of Archaeological Science* 37(7): 1557–1563.

Klein, R.G. 1984. The large mammals of southern Africa: late Pliocene to Recent. In: Klein, R.G. (ed.) *Southern African Prehistory and Paleoenvironments*: 107–146. Rotterdam and Boston: A.A. Balkema.

Le Baron, J.C., Kuman, K. & Grab, S.W. 2010. The landscape distribution of Stone Age artefacts on the Hackthorne plateau, Limpopo River Valley, South Africa. *South African Archaeological Bulletin* 65(192): 123–131.

Lombard, M., Bradfield, J., Caruana, M.V., Makhubela, T.V., Dusseldorp, G.L., Kramers, J.D. & Wurz, S. 2022. The southern Afri-

can Stone Age sequence updated (II). *South African Archaeological Bulletin* 77: 172–212.
Lukich, V. & Ecker, M. 2022. Pleistocene environments in the southern Kalahari of South Africa. *Quaternary International* 614: 50–58.
Lyman, R.L. 2012. *Quantitative Paleozoology*. Cambridge: Cambridge University Press.
Lyons, R., Tooth, S. & Duller, G.A.T. 2014. Late Quaternary climatic changes revealed by luminescence dating, mineral magnetism and diffuse reflectance spectroscopy of river terrace palaeosols: a new form of geoproxy data for the southern African interior. *Quaternary Science Reviews* 95: 43–59.
Macphail, R.I. & Goldberg, P. 2017. *Applied Soils and Micromorphology in Archaeology*. Cambridge: Cambridge University Press.
Marshall, T.R. & Harmse, J.T. 1992. A review of the origin and propagation of pans. *South African Geographer* 19: 9–21.
Mercier, N. & Falguères, C. 2007. Field gamma dose-rate measurement with a NaI(Tl) detector: re-evaluation of the "threshold" technique. *Ancient TL* 25(1): 1–4.
Mitchell, P.J. 1990. A palaeoecological model for archaeological site distribution in southern Africa during the Upper Pleniglacial and Late Glacial. In: Gamble, C. & Soffer, O. (eds) *The World at 18000 BP*: 189–205. London: Unwin Hyman.
Mitchell, P.J. 2000. The organization of Later Stone Age lithic technology in the Caledon Valley, southern Africa. *African Archaeological Review* 17(3): 141–176.
Mitchell, P.J. 2016. Later Stone Age hunter-gatherers and herders. In: Knight, J. & Grab, S.W. (eds) *Quaternary Environmental Change in Southern Africa: Physical and Human Dimensions*: 385–396. Cambridge: Cambridge University Press.
Mitchell, P.J. 2017. Discontinuities in hunter-gatherer prehistory in southern African drylands. *Journal of Anthropological Archaeology* 46: 40–52.
Mulholland, S.C. & Rapp, G.J. 1992. *Phytolith Systematics*. *Emerging Issues*. New York: Plenum Press.
Murray, A.S. & Wintle, A.G. 2000. Luminescence dating of quartz using an improved single-aliquot regenerative-dose protocol. *Radiation Measurements* 32(1): 57–73.
Neumann, K., Strömberg, C.A.E., Ball, T., Albert, R.M., Vrydaghs, L. & Scott Cummings, L. 2019. International Code for Phytolith Nomenclature (ICPN) 2.0. *Annals of Botany* 124: 189–199.
Palmison, M.E. 2014. Excavation, analysis, and intersite comparison of the Robberg industry components at the open-air site of Erfkroon, South Africa. Unpublished MA thesis. San Marcos, Texas State University.
Prescott, J.R. & Hutton, J.T. 1994. Cosmic ray contributions to dose rates for luminescence and ESR dating: large depths and long-term time variations. *Radiation Measurements* 23(2): 497–500.
Regev, L., Steier, P., Shachar, Y., Mintz, E., Wild, E.M., Kutschera, W. & Boaretto, E. 2017. D-REAMS: a new compact AMS system for radiocarbon measurements at the Weizmann Institute of Science, Rehovot, Israel. *Radiocarbon* 59: 775–784.
Rhodes, S.E., Goldberg, P., Ecker, M., Horwitz, L.K., Boaretto, E. & Chazan, M. 2022. Exploring the Later Stone Age at a micro-scale: new high-resolution excavations at Wonderwerk Cave. *Quaternary International* 614: 126–145.
Richard, M., Pons-Branchu, E., Carmieli, R., Kaplan-Ashiri, I., Alvari Gallo, A.I., Ricci, G., Caneve, L., Wroth, K., Dapoigny, A., Tribolo, C., Boaretto, E. & Toffolo, M.B. 2022. Investigating the effect of diagenesis on ESR dating of Middle Stone Age tooth samples from the open-air site of Lovedale, Free State, South Africa. *Quaternary Geochronology* 69: 101269.
Roberts, R.G., Galbraith, R.F., Yoshida, H., Laslett, G.M. & Olley, J.M. 2000. Distinguishing dose populations in sediment mixtures: a test of single-grain optical dating procedures using mixtures of laboratory-dosed quartz. *Radiation Measurements* 32(5): 459–465.
Rossouw, L. 2006. Florisian mammal fossils from erosional gullies along the Modder River at Mitasrust farm, central Free State, South Africa. *Navorsinge van die Nasionale Museum Bloemfontein* 22(6): 145–161.
Sampson, C.G. 1985. *Atlas of Stone Age Settlement in the Central and Upper Seacow Valley*. Bloemfontein: National Museum.
Sampson, C.G., Moore, V., Bousman, C.B., Stafford, B., Giordano, A. & Willis, M. 2015. A GIS analysis of the Zeekoe Valley Stone Age archaeological record in South Africa. *Journal of African Archaeology* 13(2): 167–185.
Sampson, G. 1970. *The Smithfield Industrial Complex: Further Field Results*. Bloemfontein: National Museum.
Scott, L., Van Aardt, A.C., Brink, J.S., Toffolo, M.B., Ochando, J. & Carrión, J.S. 2019. Palynology of Middle Stone Age spring deposits in grassland at the Florisbad hominin site, South Africa. *Review of Palaeobotany and Palynology* 265: 13–26.
Sealy, J. 2016. Cultural change, demography, and the archaeology of the last 100 kyr in southern Africa. In: Jones, S.C. & Stewart, B.A. (eds) *Africa from MIS 6-2*: 65–76. Dordrecht: Springer.
Sewell, L., Merceron, G., Hopley, P.J., Zipfel, B. & Reynolds, S.C. 2019. Using springbok (*Antidorcas*) dietary proxies to reconstruct inferred palaeovegetational changes over 2 million years in southern Africa. *Journal of Archaeological Science: Reports* 23: 1014–1028.
Shaw, C.L. 2022. An evaluation of the infrared 630 cm^{-1} OH libration band in bone mineral as evidence of fire in the archaeological record. *Journal of Archaeological Science: Reports* 46: 103655.
Shaw, M., Ames, C.J.H., Phillips, N., Chambers, S., Dosseto, A., Douglas, M., Goble, R., Jacobs, Z., Jones, B., Lin, S.C-H., Low, M.A., McNeil, J-L., Nasoordeen, S., O'Driscoll, C.A., Saktura, R.B., Sumner, T.A., Watson, S., Will, M. & Mackay, A. 2019. The Doring River Archaeology Project: approaching the evolution of human land use patterns in the Western Cape, South Africa. *PaleoAnthropology* 2019: 400–422.
Stewart, B.A. & Mitchell, P.J. 2018. Late Quaternary palaeoclimates and human-environment dynamics of the Maloti-Drakensberg region, southern Africa. *Quaternary Science Reviews* 196: 1–20.
Stewart, B.A., Parker, A.G., Dewar, G., Morley, M.W. & Allott, L.F. 2016. Follow the Senqu: Maloti-Drakensberg paleoenvironments and implications for early human dispersals into mountain systems. In: Jones, S.C. & Stewart, B.A. (eds) *Africa from MIS 6-2*: 247–272. Dordrecht: Springer.
Stoops, G. 2021. *Guidelines for Analysis and Description of Soil and Regolith Thin Sections*, second edn. Wiley.
Stoops, G., Marcelino, V. & Mees, F. 2018. *Interpretation of Micromorphological Features of Soils and Regoliths*, second edn. Oxford: Elsevier.
Thomsen, K.J., Murray, A.S., Buylaert, J.P., Jain, M., Hansen, J.H. & Aubry, T. 2016. Testing single-grain quartz OSL methods using sediment samples with independent age control from the Bordes-Fitte rockshelter (Roches d'Abilly site, Central France). *Quaternary Geochronology* 31: 77–96.
Toffolo, M.B., Brink, J.S. & Berna, F. 2015. Bone diagenesis at the Florisbad spring site, Free State Province (South Africa): implications for the taphonomy of the Middle and Late Pleistocene faunal assemblages. *Journal of Archaeological Science: Reports* 4: 152–163.
Toffolo, M.B., Brink, J.S. & Berna, F. 2019. Microstratigraphic reconstruction of formation processes and paleoenvironments at the Early Pleistocene Cornelia-Uitzoek hominin site, Free State Province, South Africa. *Journal of Archaeological Science: Reports* 25: 25–39.
Toffolo, M.B., Brink, J.S., Van Huyssteen, C. & Berna, F. 2017. A microstratigraphic reevaluation of the Florisbad spring site, Free State Province, South Africa: formation processes and paleoenvironment. *Geoarchaeology* 32(4): 456–478.
Tooth, S., Hancox, J.P., Brandt, D., McCarthy, T.S., Jacobs, Z. & Woodborne, S. 2013. Controls on the genesis, sedimentary architecture, and preservation potential of the dryland alluvial successions in stable continental interiors: insights from the incising Modder River, South Africa. *Journal of Sedimentary Research* 83: 541–561.
Trower, G. 2010. An investigation into the archaeological, palaeontological and stratigraphic continuity between two sections of the Free State's Modder River, observed within selected erosional gullies (dongas). Unpublished MSc dissertation. Bloemfontein: University of the Free State.
Van Couvering, J.A. & Delson, E. 2020. African land mammal ages. *Journal of Vertebrate Paleontology* 40(5): e1803340.
Van der Marel, H.W. & Beutelspacher, H. 1976. *Atlas of Infrared Spectroscopy of Clay Minerals and their Admixtures*. Amsterdam: Elsevier Scientific Publishing Company.
Van Hoepen, E.C.N. 1932. Die Mosselbaaise Kultuur. *Argeologiese Navorsing van die Nasionale Museum Bloemfontein* 1: 27–54.
Von den Driesch, A. 1976. *A Guide to the Measurement of Animal Bone from Archaeological Sites*. Cambridge: Peabody Museum Press.
Wadley, L. 1993. The Pleistocene Later Stone Age south of the Limpopo River. *Journal of World Prehistory* 7: 243–296.
Weiner, S. 2010. *Microarchaeology. Beyond the Visible Archaeological Record*. New York: Cambridge University Press.
Wroth, K., Tribolo, C., Bousman, C.B., Kolska Horwitz, L., Rossouw, L., Miller, C.E. & Toffolo, M.B. 2022. Human occupation of the semi-arid grasslands of South Africa during MIS 4: new archaeological and paleoecological evidence from Lovedale, Free State. *Quaternary Science Reviews* 283: 107455.